

Gas-Expanded Liquids

Philip G. Jessop*[†] and Bala Subramaniam[‡]

Department of Chemistry, Queen's University, Kingston, Ontario, Canada K7L 3N6, and Center for Environmentally Beneficial Catalysis, Department of Chemical & Petroleum Engineering, University of Kansas, Lawrence, Kansas 66045-7609

Received August 8, 2006

Contents

1. Introduction	2666	3.6. Switchable Solvents	2682
2. Expansion and the Consequences Thereof	2668	3.7. Uncatalyzed Reactions	2683
2.1. Solubility of CO ₂ in Liquids	2668	3.7.1. Using Expansion To Shift Equilibria	2683
2.2. Equipment for Measuring Phase Behavior and Expansion	2669	3.7.2. Using Expansion To Promote Polymerization	2683
2.3. Partial Molar Volumes and Solvent Structure	2669	3.8. Homogeneous Catalysis	2683
2.4. Property Changes	2670	3.8.1. Hydrogenation	2683
2.4.1. Polarity and Hydrogen-Bonding Ability	2670	3.8.2. Hydroformylation	2684
2.4.2. Melting Point	2670	3.8.3. Oxidation Using O ₂	2685
2.4.3. Transport Properties	2671	3.8.4. Oxidation Using H ₂ O ₂	2685
2.4.4. Conductivity	2672	3.8.5. Polymerization	2686
2.4.5. Acidity	2673	3.9. Heterogeneous Catalysis	2686
2.5. Solubility Changes	2673	3.9.1. Hydrogenations	2686
2.5.1. Solubility of Solids	2673	3.9.2. Selective Oxidations	2687
2.5.2. Solubility of Reagent Gases	2674	3.9.3. Hydroformylation	2687
2.5.3. Miscibility Changes	2675	3.9.4. Solid Acid Catalysis	2687
2.6. Modeling	2676	3.10. Acid-Catalyzed Reactions	2687
2.6.1. Simulation of Compressible Gas Solubility in Liquid Solvents	2676	3.11. Other Applications	2688
2.6.2. Simulation of Permanent Gas Solubility in Expanded Liquids	2677	4. Process Engineering Issues	2688
2.6.3. Transport Properties	2677	5. Summary	2690
2.6.4. Macroscopic Models of Mixing and Reactors	2678	6. Abbreviations	2690
3. Applications	2678	7. Acknowledgment	2691
3.1. Particle Formation	2678	8. References	2691
3.1.1. Particles from Gas-Saturated Solution (PGSS)	2679		
3.1.2. Gas Antisolvent (GAS)	2679		
3.1.3. Precipitation with Compressed Antisolvent (PCA) and Aerosol Solvent Extraction System (ASES)	2679		
3.1.4. Solution-Enhanced Dispersion by Supercritical Fluids (SEDS)	2679		
3.1.5. Depressurization of an Expanded Liquid Organic Solution (DELOS)	2679		
3.1.6. Precipitation of Particles from Reverse Emulsions	2680		
3.1.7. Particle Processing	2680		
3.2. Enhanced Oil Recovery	2680		
3.3. Polymer Processing	2680		
3.4. Separations and Crystallizations	2681		
3.5. Postreaction Separations	2681		

1. Introduction

Solvent usage has been linked to waste generation and associated environmental and economic burdens. Table 1 compares the amount of waste generated relative to products formed (this ratio is the so-called environmental burden index or *E-factor*)¹ in various chemical industry sectors. Even though the oil refining and petrochemical industries generate large amounts of waste in absolute terms, their *E-factor* is the lowest. In contrast, the *E-factor* varies from 25 to 100, or in many cases, far higher, as in the case of the pharmaceutical and specialty chemicals sectors, even though the production scales are significantly lower. Solvents are to blame for much of this excessive wastage.

In addition to creating liquid wastes that must be properly handled and disposed of, conventional solvents readily evaporate. Industrial processing operations release 20 million tons of volatile organic carbons (VOCs) per year.² Solvents make up two-thirds of all industrial emissions and one-third of all VOC emissions in the United States. The solvent emissions have been linked to poor air quality and human illness. Consequently, many chemical companies have incorporated responsible environmental stewardship as part of their mission. The major targets to reduce environmental and cost burdens in conventional processes include signifi-

* To whom correspondence should be addressed. E-mail: jessop@chem.queensu.ca.

[†] Queen's University.

[‡] University of Kansas.



Dr. Jessop is Canada Research Chair of Green Chemistry at Queen's University in Kingston, Ontario, Canada. He received his Ph.D. in Inorganic Chemistry from the University of British Columbia in 1991. After a postdoctoral appointment at the University of Toronto, he took a contract research position in the Research Development Corp. of Japan in a project headed by Ryoji Noyori (Nobel Prize 2001), investigating hydrogenations in supercritical CO₂. An assistant professor at the University of California-Davis from 1996 to 2003, he was awarded a Canada Research Chair position at Queen's University from 2003. In 2004 he received the Canadian Catalysis Lectureship Award from the Canadian Catalysis Foundation. His research interests include chemical reactions in unusual solvents (supercritical fluids, ionic liquids, gas-expanded liquids, and switchable solvents), the conversion of CO₂ to useful products, and chemistry related to H₂ storage.



Dr. Bala Subramaniam earned his Ph.D. in chemical engineering from the University of Notre Dame. He is currently the Dan F. Servey Distinguished Professor of Chemical Engineering and the Director of the Center for Environmentally Beneficial Catalysis, a National Science Foundation Engineering Research Center, at the University of Kansas (KU). He has held visiting Professorships at ETH in Zurich, Switzerland, and at the University of California, Davis. Dr. Subramaniam serves on the editorial board of *Applied Catalysis B: Environmental*. He has received several awards including the Dow Outstanding Young Faculty Award from the American Society for Engineering Education and a Higuchi Research Achievement Award from KU. Dr. Subramaniam's research interests are in catalytic reaction engineering, crystallization, and exploiting supercritical fluids and gas-expanded liquids for benign chemicals processing.

cant reduction of solvent usage and replacement with benign alternatives.

During the last two decades, many research groups have been active at finding alternate media for performing chemical reactions.^{3–6} Supercritical CO₂ (scCO₂),^{7–13} water,^{14,15} CO₂-expanded liquids (CXLs), ionic liquids (ILs),^{16,17} and switchable solvents¹⁸ have received much attention as benign media. The application of supercritical CO₂ as a benign medium in chemistry and reaction engineering satisfies several green chemistry and engineering principles

Table 1. Per Capita Waste Generation in Chemical Industry Sectors^{1a}

industry sector	product tonnage/yr	kg byproducts/kg product
Oil refining	10 ⁶ –10 ⁸	ca 0.1
Bulk Chemicals	10 ⁴ –10 ⁶	<15
Fine Chemicals	10 ² –10 ⁴	1–50
Pharmaceuticals	10 ¹ –10 ³	25–100+

^a Reprinted with permission from ref 1. Copyright 1994 American Chemical Society.

such as pollution prevention, lower toxicity, and use of an “abundantly available” resource with no increase in environmental burden. However, the reaction rate benefits are often marginal with scCO₂ (except for reactions that are kinetically dependent on reactant gases and/or are mass transfer-limited). In many cases, scCO₂-based reactions are limited by inadequate solubilities of reagents or catalysts. Additionally, CO₂ is nonpolar, which results in relatively low reaction rates for reactions that have polar transition states. Furthermore, high process pressures (well over 100 bar) are required. The combination of high pressures and, for some reactions, low reaction rates increases energy consumption and reactor volumes, both of which adversely affect process economics and decrease the environmental advantages. In contrast, the use of organic solvents offers important reaction benefits. For example, solvents are typically chosen with dielectric properties that help solubilize the reagents and/or homogeneous catalysts and improve the rate of the desired reaction. However, the concerns with conventional organic solvents are toxicity and environmentally deleterious vapor emissions that may also form explosive mixtures with air. As detailed in this review, expanded liquids combine the beneficial properties of compressed gases such as CO₂ and of traditional solvents, leading to a new class of tunable solvents that are often the ideal type of solvents for a given application while simultaneously reducing the environmental burden.

In recent years, several research groups have clearly demonstrated how these relatively new solvents, called gas-expanded liquids (GXLs), are promising alternative media for performing separations, extractions, reactions, and other applications. A GXL is a mixed solvent composed of a compressible gas (such as CO₂ or ethane) dissolved in an organic solvent. Because of the safety and economic advantages of CO₂, CO₂-expanded liquids (CXLs) are the most commonly used class of GXLs. By varying the CO₂ composition, a continuum of liquid media ranging from the neat organic solvent to scCO₂ is generated, the properties of which can be adjusted by tuning the operating pressure; for example, a large amount of CO₂ favors mass transfer and, in many cases, gas solubility, and the presence of polar organic solvents enhances the solubility of solid and liquid solutes. CXLs have been shown to be optimal solvents in a variety of roles including inducing separations, precipitating fine particles, facilitating polymer processing, and serving as reaction media for catalytic reactions. *Process advantages* include ease of removal of the CO₂, enhanced solubility of reagent gases (compared to liquid solvents), fire suppression capability of the CO₂, and milder process pressures (tens of bars) compared to scCO₂ (hundreds of bars). *Reaction advantages* include higher gas miscibility compared to organic solvents at ambient conditions, enhanced transport rates due to the properties of dense CO₂, and between 1 and 2 orders of magnitude greater rates than in neat organic

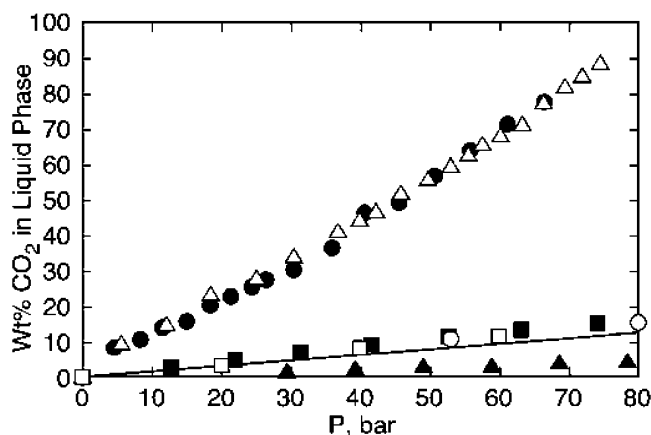


Figure 1. The mass fraction solubility of CO₂ in Class I (water,³³⁷ (▲), Class II (ethyl acetate²⁴ (●) and MeCN²⁴ (Δ)), and Class III liquids ([bmim]BF₄⁴¹ (■), crude oil²²² (UOP $K = 11.7$, assuming MW of 350, shown as a line), PEG⁴² (O), and PPG⁴² (□)). “bmim” is 1-*n*-butyl-3-methylimidazolium. All data are for 40 °C, except water and PPG at 35 °C and oil at 43 °C. Note that not all Class II liquids follow the same line as ethyl acetate and MeCN; a lower line is taken by DMF, for example (not shown).

solvent or *sc*CO₂. *Environmental advantages* include substantial replacement of organic solvents with environmentally benign dense-phase CO₂. Thus, CXLs have emerged as important components in the optimization of chemical processes.

There are some related terms that may cause confusion. The term “expanded liquids” is also used for liquid metals (Hg, Cs, Cd) which are expanded by heating,¹⁹ but those liquids are not within the scope of this review. The term “enhanced fluidity liquids” has also been used in the literature^{20,21} for mixtures of solvents and CO₂ used as HPLC mobile phases for chromatographic separations. These mixtures are often far above the bubble point with pressures typical of supercritical fluid processing. In other words, an “enhanced fluidity liquid” resembles a supercritical fluid more than a GXL.

2. Expansion and the Consequences Thereof

2.1. Solubility of CO₂ in Liquids

As CO₂ (or any compressible gas) dissolves into an organic liquid, the liquid expands volumetrically, forming a GXL. Not all liquids expand equally in the presence of CO₂ pressure, and the differences in behavior are attributed to differences in the ability of the liquids to dissolve CO₂. In this regard, liquids can be divided into three general classes,²² and there is variation within the classes.

Class I liquids such as water have insufficient ability to dissolve CO₂ (Figure 1) and, therefore, do not expand significantly and have essentially no change in their properties, except acidity. Although there is a lack of data, one would expect glycerol and other polyols to fall into this class. However, by the use of a solvent such as acetonitrile or methanol that exhibits mutual solubility in CO₂ and water, it is possible to create CO₂-expanded ternary systems containing water.²³

Class II liquids, such as methanol, hexane, and most other traditional organic solvents, dissolve large amounts of CO₂ (Figure 1), expand greatly (Figure 2), and consequently undergo significant changes in virtually every physical property. CO₂ solubility in class II liquids is traditionally

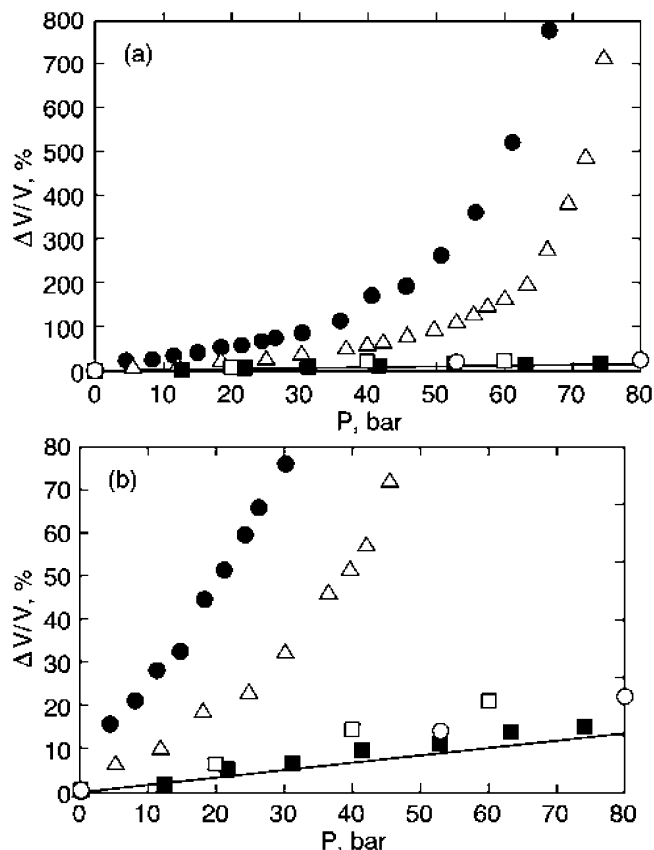


Figure 2. Expansion of solvents as a function of the pressure of CO₂ at 40 °C, for ethyl acetate (●),²⁴ MeCN (Δ),²⁴ [bmim]BF₄ (■),⁴¹ crude oil (line, at 43 °C),²²² PEG (□),⁴² and PEG (O).⁴² The [bmim]BF₄ data is interpolated from the literature data.

Table 2. A Comparison of Different Classes of Solvents²² and Their Expansion Behavior at 40 °C under CO₂ Pressure^a

class	solvent	P , bar	volumetric expansion, %	wt % CO ₂	mol % CO ₂	ref
I	H ₂ O	70	na	4.8	2.0	40
II	MeCN	69	387	83	82	24
	1,4-dioxane	69	954	79	89	24
	DMF	69	281	52	65	24
III	[bmim]BF ₄ ^a	70	17	15	47	41
	PEG-400	80	25	16	63	42
	PPG-2700 ^b	60	25	12	89	42

^a Interpolated from the literature data. ^b At 35 °C.

depicted on a mole% basis, because volumetric expansion of class II solvents is dependent only on the mole fraction of CO₂ in the liquid phase and independent of the choice of solvent.²⁴

Class III liquids, such as ionic liquids, liquid polymers, and crude oil, dissolve only moderate amounts of CO₂ (Figure 1) and, therefore, expand only moderately in volume (Figure 2). As a result, some properties such as viscosity change significantly while others, such as polarity, do not. The degree to which CO₂ is soluble in class III liquids is much greater on a mole% basis than on a mass% basis (Table 2). For liquids that have a much higher molecular weight (e.g., liquid polymers)²⁵ than CO₂ or for liquids having variable molecular weight (e.g., crude oil), mass% data is more useful for comparisons. The failure of class III solvents to expand is primarily due to their poor ability to dissolve CO₂ and not because of an inability to expand in proportion to the amount of CO₂ dissolved. Plotting expansion as a

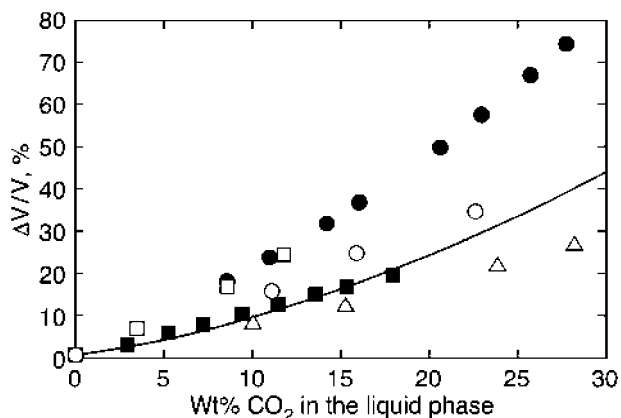


Figure 3. Expansion of liquids at 40 °C, as a function of the mass fraction of CO₂ dissolved in MeCN (Δ),²⁴ ethyl acetate (●),²⁴ [bmim]BF₄ (■),⁴¹ crude oil (line),²²² PPG (□),⁴² and PEG (○).⁴² The [bmim]BF₄ data is interpolated from the literature data. All data are for 40 °C, except PPG at 35 °C and crude oil at 43 °C.

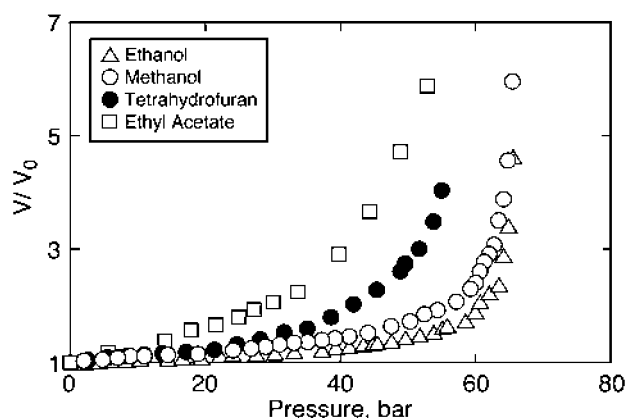


Figure 4. Isothermal volumetric expansion of benign solvents by CO₂ at 40 °C.³⁸

function of CO₂ mass fraction in the liquid phase (Figure 3) shows that the ionic liquids and liquid polymers expand as much as class II solvents, at equal CO₂ content.

High pressure vapor–liquid equilibria (VLE) data for fluid mixtures containing organic liquids and compressed CO₂ are relatively abundant in literature. Miscibility of CO₂ has been investigated experimentally with a variety of class II liquids including alkanes, alcohols, aromatics, ketones, and esters, among others.^{24,26–31} Experimental VLE data of many CO₂ and organic binary and ternary systems are available in several reviews.^{32–36}

The miscibility of dense CO₂ with class II solvents has also been modeled.^{24,37} The miscibility as observed by an expansion of the liquid mixtures by CO₂ is recorded in terms of the relative increase in the liquid volume from the initial state (CO₂-free, atmospheric pressure, P^0) to the final state (CO₂-expanded, equilibrated pressure, P) at the same temperature. Figure 4 shows the isothermal volumetric expansion of some class II solvents by CO₂.³⁸ Clearly, CO₂ is soluble to varying degrees in the solvents. These expansions are successfully predicted by the Peng–Robinson Equation of State (PR-EoS) and molecular simulations (discussed in section 2.6.1). For all of these solvents, a 2- to 3-fold volumetric expansion is observed at relatively mild pressures (50–60 bar). In other words, CXLs may be created at relatively mild pressures with a substantial replacement of the organic solvent with CO₂.

Gases such as ethane, fluoroform and other compressible gases are also capable of expanding liquids and can sometimes differ from CO₂ in the effect of the expansion on chemistry taking place in the liquid.³⁹ Noncompressible gases (i.e., those having critical temperatures far below the temperature of the experiment) are generally incapable of expanding solvents.

2.2. Equipment for Measuring Phase Behavior and Expansion

There are many types of experimental apparatus for studying high-pressure fluid phase equilibria. The central unit of the apparatus is a view cell, whose volume may be fixed or variable, depending on the experimental design. For example, variable-volume view cells are suitable for obtaining bubble and dew points at constant feed compositions; while fixed-volume view cells are often used for monitoring the volume expansion of the liquid phase upon CO₂ addition. Mixing is generally provided by stirring the system with a magnetic stirrer, or by circulating the liquid or vapor phase with a recirculating pump. An example of the variable-volume circulation apparatus is reported by Radosz.⁴³ The fluid density can be monitored with an in-line densitometer, while the composition data are obtained via a sampling device that connects to a gas chromatograph.

Volumetric expansion measurements are typically performed in a Jerguson-type view cell as described elsewhere.⁴⁴

Recently, an optical fiber probe has been developed for *in situ* monitoring of volume changes in CO₂-expanded solvents.⁴⁵ This is a variation of the probe developed by Xue et al.⁴⁶ The optical probe uses the difference in the refractive index of liquid, gas, and optical fiber to distinguish between the vapor and the expanded liquid phase for volume expansion measurement; and between two phases and supercritical (single phase) condition for phase transition measurement. The *in situ* probe is particularly useful for detecting changes in GXL phase volume in large-scale vessels that do not have windows for visual detection.

2.3. Partial Molar Volumes and Solvent Structure

The fundamental principles developed for gas-phase or liquid-phase reactions may be applied to supercritical and GXL phases as well. When the reaction medium density is gas-like, the concepts developed for gas-phase reactions (such as kinetic theory of gases) may be applied. For liquid-like reaction mixtures (i.e., dense supercritical reaction media), principles of liquid-phase kinetics are applied. Parameters such as the solvent's solubility parameter, dielectric constant, or solvatochromic shift, routinely used to interpret liquid-phase reactions, have been employed to understand the effect of a given solvent on chemical reaction.

The transition from a GXL to a supercritical fluid (SCF) may be viewed as follows. As a GXL approaches a SCF, the rate of volume expansion increases dramatically with pressure. As the critical point of the mixture is reached (typically at greater than 90% CO₂), the vapor and liquid phases merge giving rise to a cosolvent-modified SCF. Molecular simulations^{47–49} indicate that significant changes to the sorting of the liquid and CO₂ structure occur for mole fractions of CO₂ greater than approximately 0.5. In the case of the C₆H₁₂ + CO₂ system, the mixing appears to be almost completely random even at CO₂ mole fractions >0.9. In contrast, in polar CXLs such as CH₃CN + CO₂ and

especially in associating $\text{CH}_3\text{OH} + \text{CO}_2$ CXLs, significant solvent sorting occurs. Despite these structural differences, the thermodynamic and dynamic properties are similar in all these CXLs. The presence of CO_2 is far more effective at inducing clustering of methanol molecules than non-hydrogen bonding acetone molecules.

When compressed CO_2 is dissolved in an ionic liquid, its partial molar volume is much smaller than that observed in most other solvents. The possible causes for this behavior have been the subject of several experimental and computational investigations. Employing IR studies, Kazarian and co-workers⁵⁰ found no evidence of specific interaction of CO_2 with the imidazolium cation, indicating that the role of acidic H attached to C_2 is not an important factor in the solubility of CO_2 . This was later confirmed by the computations of Maginn and Brennecke's groups⁵¹ who show computationally that radial distribution functions in the neat IL are essentially identical to those in the mixture, thereby concluding that the structure of the liquid is unchanged by dissolving CO_2 . The authors also propose that cations and anions form a network and CO_2 fills the interstices. Further, the ionic liquid molar volume and CO_2 solubility were correlated well through Henry's constants and other thermodynamic properties for different CO_2 -IL systems.^{52,53} Employing molecular dynamics simulations, Huang et al.⁵⁴ show that the liquid structure of [bmim][PF₆] (where "bmim" is *n*-butyl-3-methylimidazolium) in the presence of CO_2 is nearly identical to that in the neat ionic liquid (IL) even at fairly large mole fractions of CO_2 . Their simulations confirm experimental observations that while CO_2 is highly soluble in the ionic liquid phase (on a mole % basis), the ionic liquid is highly insoluble in the CO_2 phase.⁵⁵ The authors propose that even though cavity sizes in the neat IL are small compared with the van der Waals radius of a single carbon or oxygen atom, CO_2 occupies a space that was *a priori* "empty".

2.4. Property Changes

2.4.1. Polarity and Hydrogen-Bonding Ability

Solvent polarity, as measured by solvatochromic dyes, is affected by solvent expansion. One of the most common polarity measures is the Kamlett-Taft π^* parameter, which reports a combination of solvent polarity and polarizability (π^* is 1 for DMSO and 0 for cyclohexane).⁵⁶ The π^* of class II solvents drops dramatically as the CO_2 pressure increases, unless the solvent's polarity is comparable to that of CO_2 itself (Figure 5). The π^* of *scCO*₂ at 40 °C is -0.05 to $+0.15$ depending on the density.⁵⁷

The situation is quite different for class III liquids. Ionic liquids barely change in π^* even at 75 bar of CO_2 .^{58,59} Other solvatochromic measures of solvent polarity include the Nile Red scale⁶⁰ and the pyrene I_1/I_3 scale. Using the pyrene I_1/I_3 scale, Baker et al.⁶¹ confirmed that [bmim]PF₆ drops only slightly in polarity upon dissolution of CO_2 (even at 120 bar, 35 °C). Heldebrant et al.²² showed with the Nile Red dye that the polarities of liquid poly(propylene glycol) and poly(ethylene glycol) drop only gradually with increasing CO_2 pressure, but the fact that they drop contrasts with the behavior of ionic liquids.

While solvatochromic dyes measure the local polarity around solute molecules, the bulk solvent polarity is most commonly measured by the dielectric constant. The dielectric constant has not been measured for expanded liquids, but the local dielectric constant for CO_2 -expanded [bmim]PF₆

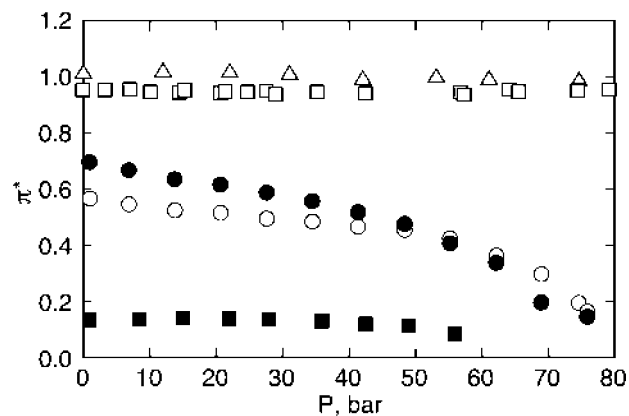


Figure 5. The dependence of π^* on the pressure of CO_2 over expanded methanol (○),³³⁸ acetone (●),³³⁸ [bmim]BF₄ (△)⁵⁹ [bmim]PF₆ (□)⁵⁸ and ethoxynonafluorobutane (■),⁸⁸ all at 40 °C except [bmim]PF₆ and ethoxynonafluorobutane at 35 °C.

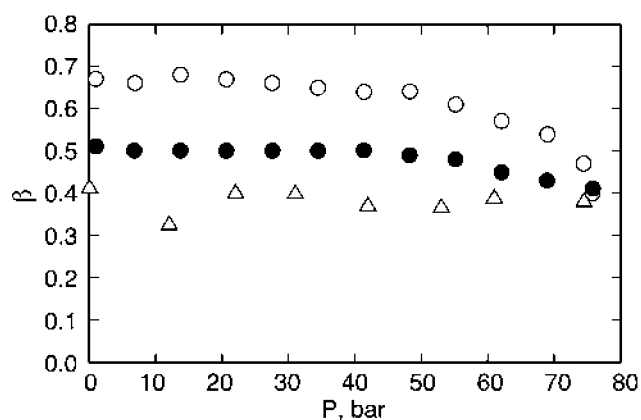


Figure 6. The dependence of β on the pressure of CO_2 over expanded methanol (○),³³⁸ acetone (●),³³⁸ and [bmim]BF₄ (△).⁵⁹ has been estimated from the fluorescence emission maximum of 9-(dicyanovinyl)julolidine. The dielectric constant was 41 at 1 bar and essentially independent of CO_2 pressure.⁵⁸

Other solvent properties such as hydrogen-bond accepting ability (quantified by the Kamlett-Taft parameter β) and especially the hydrogen-bond donating ability (the parameter α) are less strongly affected by expansion. There is a small drop in the β value of class II solvents (acetone and methanol) above 50 bar (Figure 6). Little change in the β value is seen with the ionic liquid [bmim]BF₄. The β value of pure CO_2 varies between -0.08 and $+0.06$.⁶² Hydrogen-bond-donating ability (α) is almost constant for methanol and [bmim]BF₄ and slightly increases for acetone (Figure 7).

2.4.2. Melting Point

In 1896, Paul Villard noticed that compressed ethylene gas caused camphor to liquefy below its melting point.⁶³ This phenomenon has since been found to be fairly common. The melting points of organic solids are lowered by the presence of a compressed gas, as long as the temperature is not too far above the critical temperature of the gas and the gas is soluble in the molten organic. Gases that display this effect include CO_2 , ethane, ethylene, and xenon (Figure 8). Gases such as methane that have a T_c far below the normal melting point of the organic solid are much less effective. Organic compounds that are affected include simple organic compounds, ionic liquids,⁶⁴ lipids,⁶⁵ and polymers.⁶⁶⁻⁷² The T_m decreases because of gas dissolution in the molten organic compound.

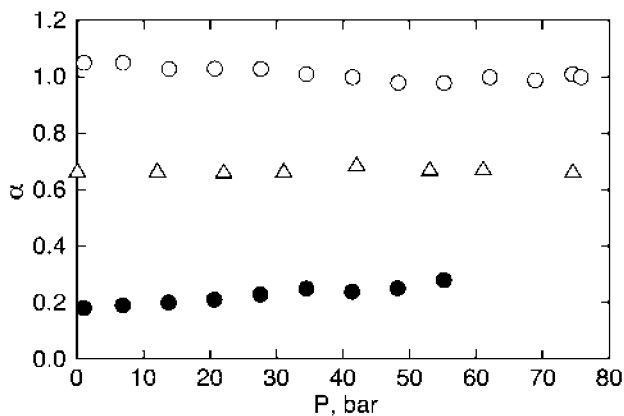


Figure 7. The dependence of α on the pressure of CO₂ over expanded methanol (○),³³⁸ acetone (●),³³⁸ and [bmim]BF₄ (△).⁵⁹

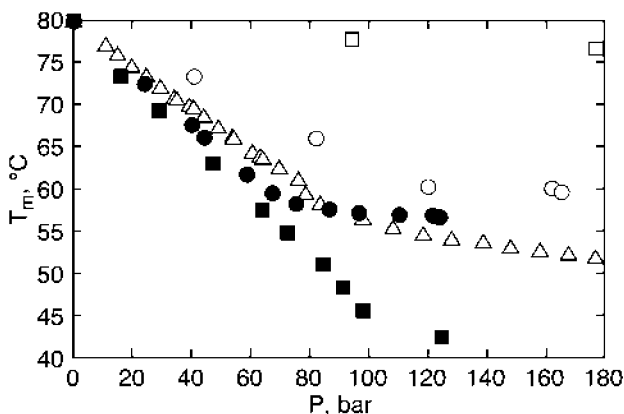


Figure 8. The effect of CO₂ (○),³³⁹ C₂H₆ (●),³⁴⁰ C₂H₄ (△),^{74,341} methane (□),³⁴² and xenon (■)³⁴³ on the melting point of naphthalene. The upper critical endpoint in ethane is 124.1 bar and 56.6 °C.³⁴⁰

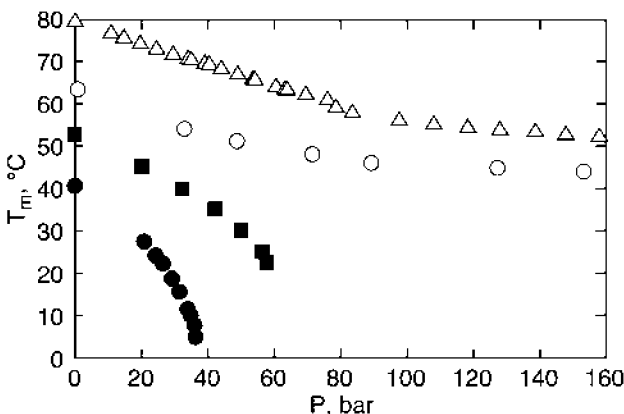


Figure 9. The effect of ethylene gas on the melting points of octacosane (○),⁷³ naphthalene (△),^{74,341} *p*-dichlorobenzene (■),⁷⁴ and menthol (●).⁷⁴

A plot of melting point versus the pressure of the expansion gas, as shown in Figures 8 and 9, is a P/T projection of the S-L-G (solid–liquid–gas) curve of the binary mixture phase diagram.⁷³ In most cases, the melting point lowering is less than 30 °C and reaches a limit caused by the occurrence of an upper critical end point on the S-L-G curve, although many of the curves flatten out before the end point is reached. Some compounds, such as biphenyl and octacosane (with CO₂ as the expansion gas) pass through a temperature minimum, after which further increases in pressure cause a rise in the melting point. For a few gas/

solid combinations, no upper critical end point exists, and the melting point lowering can be substantially greater (for example, menthol and *p*-dichlorobenzene in Figure 9).⁷⁴ The lack of an end point, and hence the greatest drop, is most likely to occur if the T_c of the gas is very close to, or even above, the T_m because the gases, being highly compressible at such temperatures, are more soluble in the organic compound. For example, pentane (T_c 197 °C) lowers the melting point of anthracene (T_m 218 °C) without an end point, while ethane (T_c 32 °C) has only a moderate effect on the T_m .⁷⁵ Gases that are only moderately soluble in the liquid depress the T_m only slightly,⁷⁶ while gases that are very poorly soluble (such as N₂ in liquid naphthalene)⁷⁷ raise the T_m , just as hydrostatic pressure would.

An equation for predicting the melting point lowering has been reported, based on Raoult's law.⁷⁸

Ionic liquids seem to exhibit greater melting point depressions upon CO₂ expansion, although the data so far are limited. Tetrahexylammonium nitrate, which normally melts at 69 °C, is liquid at room temperature under CO₂ pressure.⁷⁹ Even larger melting point depressions were reported by Leitner for tetraalkylammonium and tetraalkylphosphonium ionic liquids such as tetra-*n*-butylammonium tetrafluoroborate, which melts at 156 °C at 1 bar and at 36 °C under 150 bar of CO₂, showing a melting point depression of 120 °C.^{80,81} Other ionic liquids have melting point depressions on a more modest scale (25 °C for 1-hexadecyl-3-methylimidazolium hexafluorophosphate).⁶⁴ The factors that determine the magnitude of the depression have not been identified.

Polymers show moderate changes in the T_m ,⁸² the glass transition temperature (T_g), and the crystallization temperature. For example, the T_m of polypropylene lowers by 0.12 °C/bar of CO₂, while the crystallization temperature lowers by 0.18 °C/bar.^{67,83} Poly(ethylene terephthalate)⁸⁴ has a T_m lowering of 0.042 °C/bar and a T_g lowering of 0.717 °C/bar. CO₂ also increases the rate of crystallization,⁸⁴ so that samples with high crystallinity can be obtained by annealing the polymer under CO₂ pressure.⁸⁵ The potential applications of the T_m and T_g lowering effect in organic solids and polymers include fine particle formation (section 3.1), promotion of solventless reactions of solids (sections 3.8 and 3.9) and polymer processing (section 3.3).

2.4.3. Transport Properties

Sassiat and Morier⁸⁶ reported that the diffusion coefficients of benzene in CO₂-expanded methanol are enhanced between 4- and 5-fold with CO₂ addition. Recently, Eckert's group employed the Taylor-Aris dispersion to measure diffusivities of several solutes (benzene, pyridine, pyrimidine, pyrazine, and 1,3,5 triazine) in CO₂-expanded methanol (Figure 10).⁸⁷ As expected, all solutes exhibit increased diffusivity as the CO₂ content in the CXL is increased. Further, as evident in Figure 10, differences in polarity of the solutes have an insignificant effect on the measured diffusion coefficients. The authors concluded that diffusion in CXLs is governed more strongly by physical constraints such as steric effects than by chemical interactions.

Kho et al.⁸⁸ measured viscosities of CO₂-expanded fluorinated solvents using an electromagnetic viscometer. In the 25–35 °C range and at pressures from 8 to 72 bar, Kho et al. report up to a 4- to 5-fold decrease in viscosity with CO₂ addition.

Shifflett and Yokozeki⁸⁹ measured gaseous carbon dioxide (CO₂) absorption in [bmim][PF₆] and [bmim][BF₄] using a

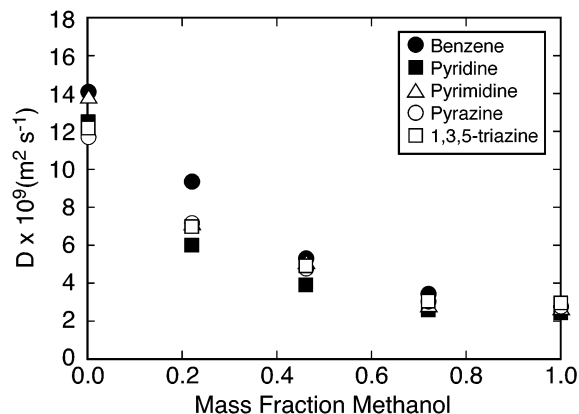


Figure 10. Diffusion coefficients of benzene, pyridine, pyrimidine, pyrazine, and 1,3,5-triazine in CO₂-expanded methanol as a function of mass fraction of methanol, at 40 °C and 150 bar.⁸⁷

gravimetric microbalance in the 10–75 °C range and at pressures under 20 bar, although it should be noted that these pressures are too low to take full advantage of the mass-transfer enhancing effects of expansion. From transient absorption data, binary diffusion coefficients of CO₂ in the ILs were estimated and found to be 10⁻¹¹–10⁻¹⁰ m² s⁻¹, which are about 10–100 times lower than typical values encountered for gas diffusion in organic liquids. Shifflett and Yokozeki⁹⁰ also reported similar measurements of hydrofluorocarbon gases (trifluoromethane, difluoromethane, pentafluoroethane, 1,1,1,2-tetrafluoroethane, 1,1,1-trifluoroethane, and 1,1-difluoroethane) in [bmim][PF₆] and [bmim][BF₄] and found large differences in the solubility among the hydrofluorocarbons. Experimental gas solubility data were successfully correlated with well-known solution models (Margules, Wilson, and NRTL activity coefficient equations). Morgan et al.⁹¹ reported diffusivity and solubility data for carbon dioxide, ethylene, propylene, 1-butene, and 1,3-butadiene in imidazolium-based ILs and a phosphonium-based IL encompassing a wide range of liquid viscosities. They also reported that gas diffusion in ILs (~10⁻¹⁰ m² s⁻¹) is slower than that in traditional hydrocarbon solvents and water. A correlation for gas diffusivity in ILs was proposed in terms of the gas molar volume, the IL viscosity, and density. Kukova et al.⁶⁸ reported that the diffusion coefficients of CO₂ in PEG melts are in the range of 10⁻¹⁰–10⁻⁹ m² s⁻¹.

Compressed CO₂ reduces the viscosity of ILs as well. Liu et al.⁹² investigated the viscosity of CO₂-saturated [bmim][PF₆] and CO₂/[bmim][PF₆]/methanol ternary mixture at 40 °C and at 70–100 bar, pressures high enough to have a significant impact. They found that, while the viscosity of the CO₂/[bmim][PF₆] decreases by up to 3-fold with increasing CO₂ content, the viscosity of the ternary mixture varies less with composition. Eckert's group⁵⁸ investigated the solvent properties of mixtures of [bmim][PF₆] and CO₂ as functions of temperature (35–50 °C) and CO₂ pressure (0–230 bar) and reported that the microviscosity in the vicinity of the solute was reduced by more than 4-fold in CO₂-saturated ILs relative to the neat IL.

Viscosity changes upon CO₂ introduction are also dramatic in the case of polymers. Dissolving gases in polymers significantly alters the rheology of the resulting polymer melts lowering viscosities. The dissolution of compressed CO₂ in a polymer causes its plasticization even at low temperatures (see section 2.4.2).^{93–98} which results in a significant reduction in the viscosity of the polymer melt.⁹⁹

The use of compressed gases such as CO₂ allows processing of polymers at milder temperatures (avoiding polymer degradation) and has been investigated for many applications including polymer modification, formation of polymer composites, polymer blending, microcellular foaming, particle production, and polymerization (applications discussed in sections 3.1, 3.3, and 3.8). During the past decade, rheological studies of polymer/CO₂ solutions has received increased attention. Tomasko et al.¹⁰⁰ and Nalawade et al.¹⁰¹ provide a detailed review of the experimental and theoretical studies of solubilities and viscosities of several polymer melts containing dissolved CO₂.

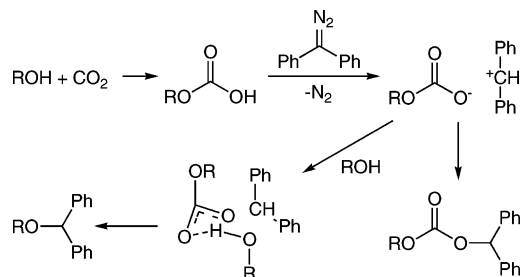
For high-pressure rheological measurements of polymer + compressed gas melts, various types of rheometers are employed such as a modified capillary extrusion rheometer,^{99,102} extrusion slit die rheometer,¹⁰³ a magnetically levitated sphere rheometer,¹⁰⁴ a rotational viscometer,¹⁰⁵ and a falling-cylinder type viscometer.¹⁰⁶ Substantial viscosity reductions have been reported for polymer melts in the presence of compressed gases. For example, Kwag et al.¹⁰² measured the viscosities of polystyrene (PS) + gas solutions containing up to 10 wt % gas [CO₂ and the refrigerants R134a (1,1,1,2-tetrafluoroethane) and R152a (1,1-difluoroethane)] and reported up to 3 orders of magnitude reduction in the Newtonian viscosity of the melts relative to pure polymer. Lee et al.^{107,108} reported that the viscosity reduction of the PE/PS blend + CO₂ melts (PE = polyethylene) lies between the values for the binary PS/CO₂ and PE/CO₂ melts. Liu et al.¹⁰⁶ report that the viscosities of low molecular weight PMMA (poly(methyl methacrylate)) solutions in acetone decreased by up to 50% in the presence of 1 wt % dissolved CO₂. Other reported rheological measurements of CO₂ + polymer melts include poly(butylene succinate) (PBS),¹⁰⁹ poly(dimethylsiloxane) (PDMS),¹⁰⁴ low-density polyethylene,¹¹⁰ poly(ethylene glycol) (PEG),⁶⁸ PMMA,¹¹⁰ polypropylene (PP),^{110,111} polystyrene,^{103,112} and poly(vinylidene fluoride) (PVDF).¹¹⁰ Whittier et al.¹¹³ report a 2 orders of magnitude reduction in the relative viscosity of PS in decahydronaphthalene in the presence of either CO₂ or SF₆. Sarrade et al.¹¹⁴ report a 5- to 500-fold reduction in the viscosities of spent oils and polymers swollen with dense CO₂. The decreased viscosity makes it possible to employ cross-flow ultrafiltration of these media to separate particulates. Viscosity reduction of crude oils upon CO₂ addition is discussed in the enhanced oil recovery section (section 3.2).

Surface tension of liquids has also shown to be dramatically reduced by dissolving gases. Hsu et al.¹¹⁵ used a pendant drop technique to measure the interfacial tension of CO₂ + *n*-butane mixtures in the 45–105 °C range at up to 80 bar. At a given temperature, the interfacial tension decreases by up to 2 orders of magnitude with increasing mole fraction of CO₂ in the liquid phase. The enhanced transport properties of GXs have been exploited in various applications, as explained in later sections.

2.4.4. Conductivity

The conductivity of ILs and viscous electrolyte solutions should, one would expect, be modified by gas expansion of the solvent because the depressed viscosity should increase ion mobility. This has been confirmed by Kanakubo et al.,¹¹⁶ who showed that the conductivity of [bmim]PF₆ increased roughly 6-fold upon the application of 100 bar of CO₂ at 40 °C. Further increase in pressure had no effect on the conductivity.

Scheme 1. Mechanism for the Formation of Ethers and Carbonates from the Reaction of Diphenyldiazomethane with CO₂-Expanded Alcohols¹²²



Although electrically conductive solids are outside the scope of this review, it is worth noting in this context that CO₂ pressure has been shown to dramatically increase the conductivity of electrolyte-containing solid polymers such as salt/PEG mixtures (MW = 500 000).¹¹⁷

2.4.5. Acidity

CO₂, when dissolved in water, lowers the pH as a function of pressure. Even though CO₂ has very poor solubility in water, the pH drops to 2.84 at 71 bar and 40 °C. At higher pressures, there is very little further change.¹¹⁸ Buffers¹¹⁹ or bases¹²⁰ can, to some extent, limit the pH drop, but high buffer concentrations are needed. The pH of high-temperature water is also lowered by the presence of CO₂.¹²¹

Alcohols behave similarly. Upon expansion with CO₂, but not other gases, acidic species form in solution. While carbonic acid monoalkyl esters are suspected, they have not been observed directly. However, chemistry associated with the presence of acids gives indirect evidence of the presence of these acids. Reichardt's solvatochromic dye is bleached in CO₂-expanded alcohols¹²² but not by alcohols alone or by CO₂-expanded aprotic solvents. A range of acid-catalyzed reactions proceed readily in CO₂-expanded alcohols but not in alcohols alone (section 3.10). The most direct evidence is the formation of methyl diphenylmethyl carbonate and methyl diphenylmethyl ether from the reaction of diphenyldiazomethane in CO₂-expanded methanol (Scheme 1).¹²² The corresponding ethyl-products were obtained in expanded ethanol.

The acidity of water or alcohols in the presence of CO₂ can be advantageous or disadvantageous, depending on the application. Enhanced acidity is obviously beneficial for acid-catalyzed reactions. The acidity of a H₂O/*sc*CO₂ biphasic system has been reported to promote the oxybromination of aromatics.¹²³ However, for colloid-catalyzed hydrogenations of arenes in a H₂O/*sc*CO₂ biphasic medium, the acidity was found to inhibit catalysis.¹¹⁹ Replacing the CO₂ with ethane solved the problem.

Emulsions containing aqueous phases are also affected by dissolved CO₂. The aqueous cores of reverse emulsions of water in iso-octane, stabilized by AOT (sodium bis-2-ethylhexylsulfosuccinate), reach a pH of 3.6 at 55 bar and 30 °C, which is not as acidic as the pH 3.2 that bulk water would have under the same pressure of CO₂. The organic continuous phase expands volumetrically as expected.¹²⁴

2.5. Solubility Changes

2.5.1. Solubility of Solids

The compressed gas in GXLs has often been exploited as an anti-solvent (as in the GAS process described in section

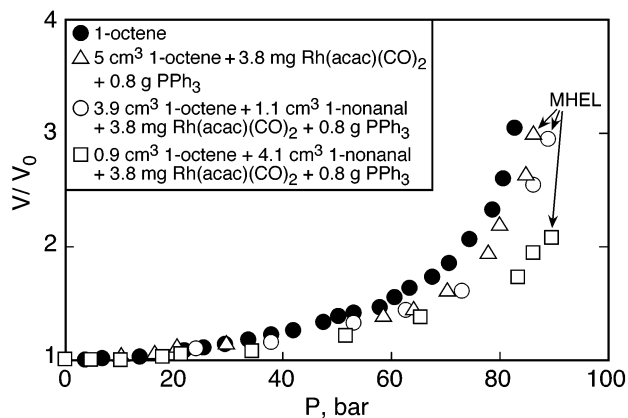


Figure 11. CO₂ expansion of representative hydroformylation reaction mixtures at 50 °C. The catalyst complex precipitates at the pressures noted. (Reprinted with permission from ref 128. Copyright 2006 Wiley Interscience).

3.1) to crystallize solutes from solution. In such applications, it is desirable to know the solid solubilities in the neat compressed gas and with added cosolvents to assess if the gas would indeed be an effective antisolvent candidate. There are more than 4500 data published for CO₂–solid solute systems, most of which are related to supercritical fluid extraction or particle formation processes.¹²⁵ The experimental apparatus for solid solubility studies contains an equilibrium cell where dense phase CO₂ is saturated with the solids at predetermined temperatures and pressures with a sampling device that allows the saturated liquid to be analyzed. The presence of a third organic component has a significant impact on the solid solubility in dense phase CO₂. Dobbs and Johnston¹²⁶ studied the cosolvent effect of methanol on the solid solubility in *sc*CO₂ at 35 °C, and observed a 3- to 4-fold enhancement in the 2-naphthol solubility with the addition of 9 mol % methanol in the system. The authors attributed the enhanced solubility to the dramatic change in the solvent polarity even with small amount of organic solvent present.

Thermodynamic models employ equations of state, and lattice gas equations (simplified correlations for the vapor-phase fugacity of a solid and its sublimation pressure assuming pure solid phase, ideal saturation, and constant volume) have been used to simulate the solubility of solids in *sc*CO₂. Recently, Mendez-Santiago and Teja¹²⁵ reported a three-parameter model developed based on the theory of dilute solutions by Harvey¹²⁷ and a Taylor expansion of the Helmholtz energy about the critical point of a solvent. The three parameters, obtained by fitting experimental data, were independent of the temperature and fluid densities up to twice of the critical density of CO₂. The model was able to predict the solubility of a solid in *sc*CO₂ with a few percent of organic cosolvent present. In the case of mixtures that contain dissolved catalysts, CO₂ addition causes catalyst precipitation at sufficiently high pressures. The liquid volume corresponding to phase separation is termed the maximum homogeneous expansion level (MHEL). The *P*–*T* region below MHEL is employed for performing homogeneous catalysis in CXLs, while the region above MHEL may be exploited for catalyst precipitation postreaction. As an example, Figure 11 compares the expansions of several hydroformylation mixtures containing 1-octene, dissolved catalyst [Rh(acac)(CO)₂ and PPh₃], and nonanals (approximating 0–20% 1-octene conversion to the nonanals).¹²⁸ As shown in Figure 11, catalyst precipitation is observed around 90 bar which demonstrates

the potential of exploiting CO₂ as an antisolvent for catalyst recovery postreaction (section 3.5).

2.5.2. Solubility of Reagent Gases

A large number of publications may be found on the vapor–liquid equilibria of H₂ (or CO) + CO₂ binary systems. Kaminishi et al.¹²⁹ and Christiansen et al.¹³⁰ reported the solubility of CO in liquid CO₂ at 10 °C. Christov and Dohrn³⁶ published a comprehensive review summarizing various high-pressure, fluid-phase equilibria for many gas (including CO₂, H₂, or CO) + organic liquid binary systems. In the range of temperatures and pressures reported in these referenced studies, the CO and H₂ solubilities in the liquid phase follow Henry's law. In contrast, relatively few publications exist that deal with H₂ (and/or CO) + CO₂ + organic liquid ternary and quaternary systems. The emerging interest in CXLs as solvent media for catalytic reactions, especially those involving gaseous reactants (such as in hydrogenation, oxidation, carbonylation, and hydroformylation), has led to increased research into the phase equilibria of (gas + CO₂ + organic/inorganic liquid) type systems.

Typically, the solubility measurements for compressed fluid systems are conducted in three ways: (1) the mass-balance method, where liquid samples are withdrawn from a vapor/liquid equilibrium cell via a sample loop, and then depressurized; the composition of the liquid mixture is obtained either by the weights before and after the volatile component is released to atmosphere, or by the pressure difference before and after the sample mixture is allowed to expand into an evacuated chamber; (2) the gas-absorption method, where agitation is provided to a system that contains a stagnant layer of compressed gas above a known amount of liquid solution; the amount of gas absorbed in the liquid is calculated based on the pressure difference before agitation and after the equilibrium is attained; (3) the direct measurement method. The third method is similar to the mass-balance method, except that instead of depressurization, the samples are vaporized in the loop through external heating and directly analyzed by a gas chromatography (GC). A fourth method, the *in situ* measurement method that recently evolved from high-pressure (HP) *in situ* characterization techniques, that is, HP-IR and HP-NMR, is perhaps the most efficient, since it requires no sampling techniques, does not disturb the equilibrium, and allows multiple analyses on the order of seconds. Dyson et al.¹³¹ measured the solubility of H₂ in several organic liquids and ILs at room temperature using an *in situ* NMR probe and compared his data with literature. However, a disadvantage of the *in situ* spectroscopic analysis is the low sensitivity compared to GC/FID techniques.

The solubilities of H₂ in CO₂-expanded 1-octene at 60 °C are presented in Figure 12a and compared to those in neat acetone at the same temperature. For H₂ + CO₂ + 1-octene ternary system, the feed gas charged into the view cell (to establish VLE) contains a premixed equimolar gas mixture of H₂ and CO₂. The H₂ mole fraction in the liquid phase is significantly enhanced in the presence of CO₂. The enhancement factors (EF, defined as the ratio of the equilibrium solubility of a gas in the CO₂-expanded liquid to that in the neat liquid at fixed vapor-phase gas fugacity) for H₂ range up to 4 at relatively mild pressures. Similar enhancement effect was reported by Hert et al.¹³² in their studies on the vapor–liquid equilibria of the O₂ (or CH₄) + CO₂ + [hmim]-[Tf₂N] system (where [hmim][Tf₂N] is 1-hexyl-3-methylimi-

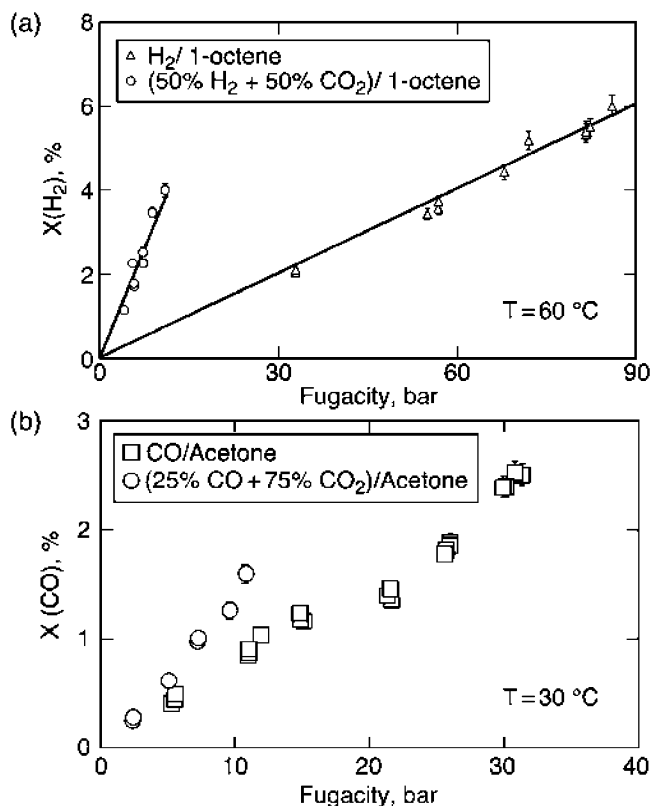


Figure 12. Solubility of H₂ and CO in neat and CO₂-expanded solvents. The x-axis represents gas-phase fugacity of (a) H₂ (b) CO.^{128,38} (Panel a reproduced with permission from ref 128. Copyright 2006 Wiley Interscience.)

dazolium bis(trifluoromethylsulfonyl)imide). Up to 5-fold solubility enhancement for O₂ and 3-fold for CH₄ occurred at pressures below 10 bar after CO₂ was introduced into the O₂ (or CH₄) + [hmim][Tf₂N] binary system.

Solinas et al.¹³³ measured the concentrations of H₂ in CO₂/IL media using an *in situ* NMR probe, and observed significant H₂ solubility enhancement upon addition of dense CO₂, which led to improved reaction rates in the enantioselective hydrogenation of imines. In addition, the mole fraction versus gas-phase fugacity behavior was nonlinear at pressures above 40 bar; the authors concluded that the pressure effect alone does not explain the observed solubility enhancement.

Bezanehtak et al.¹³⁴ reported a comprehensive study of the vapor–liquid equilibria of CO₂ + H₂ + methanol (MeOH) ternary system and observed a correlation between H₂ solubility and the critical pressures of CO₂ + MeOH, CO₂ + H₂ binary systems. The authors report that at pressures below 60 bar, the critical pressure for the CO₂+MeOH binary system, an increase in CO₂ composition led to a decrease in H₂ solubility in the liquid phase. In other words, dilution effect dominates the liquid-phase mole fraction of H₂. Above 60 bar however, the H₂ solubility increased significantly with increasing CO₂ mole fraction. This difference in the H₂ solubility behavior suggests that the interactions between CO₂ and the organic solvent may play an important role in the dissolution of H₂ in the CO₂-expanded liquid media. Xie et al.¹³⁵ reported detailed phase behavior data for the H₂ + CO₂ + methanol system with various CO₂ compositions at 40 °C and pressures up to 217 bar.

Figure 12b presents the solubility of CO in neat and CO₂-expanded acetone at 30 °C. Both sets of data follow Henry's

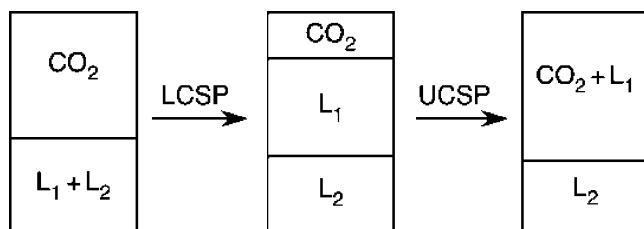


Figure 13. The phase changes observed upon expanding a mixture of two miscible liquids past a lower critical solution pressure and an upper critical solution pressure.

law in the range of pressures studied. Similar to the trend in H_2 solubility, enhancement in CO solubility upon CO_2 addition is observed in the liquid phase. Lopez-Castillo et al.¹³⁶ compared the solubility of CO in neat and CO_2 -expanded acetonitrile (26–40 °C, 40–90 bar), acetone (40 °C, 90 bar), and methanol (25 °C, 41 bar). The observed enhancement factors, ranging from 1.1 to 2.5, were similar to values reported by Jin.³⁸

Lopez-Castillo¹³⁶ also measured the solubility of O_2 in CO_2 -expanded acetonitrile, acetone, and methanol at temperatures between 25 and 40 °C, and pressures up to 90 bar. While the solubility of O_2 in CXLs is enhanced over that in the absence of CO_2 at the same O_2 fugacity, it did not substantially exceed the solubility achievable with pure O_2 at the same total pressure. However, industrial operation with pure O_2 is considered unsafe even at ambient pressures due to the risk of explosion of organic vapor/ O_2 mixtures. The fact that dilution of pure O_2 with CO_2 provides similar O_2 solubilities in the liquid phase at the same total pressure confirms the earlier hypothesis that CXLs enhance process safety.¹³⁷ This result is of practical significance.

2.5.3. Miscibility Changes

Miscible pairs of liquids can become immiscible upon expansion of the liquid phase by application of a gas (Figure 13). For example, at 40 °C, water and 1-propanol are completely miscible, forming a single-phase liquid mixture, but application of at least 68 bar of CO_2 causes the mixture to split into two liquid phases, a water-rich phase and an alcohol-rich phase, in addition to the CO_2 -rich gas phase (LLV behavior, Figure 13).¹³⁸ This transition occurs at the lower critical solution pressure (LCSP). If the pressure is increased further, then the upper critical solution pressure (UCSP) may be reached, at which point the alcohol-rich phase merges with the CO_2 phase, leaving only the water-rich liquid phase below a supercritical CO_2 /alcohol phase. In the example of water/1-propanol at 40 °C, this second transition occurs at 150 bar. For some mixtures, the upper and lower critical solution pressures are too close together for the LLV behavior to be practically useful (81 and 80 bar, respectively, for methanol/water at 40 °C).¹³⁹ In many cases, including water/1-propanol at some temperatures, further phase transitions occur between these two key pressures, including the formation of a third liquid phase.^{138,140} The pressures required are a function of the binary liquid mixture composition. This phase behavior has been reviewed in detail.¹⁴¹

Pairs of liquids that behave in this manner, with CO_2 as the gas, include water/organic, IL/organic,^{142,143} and IL/water¹⁴⁴ binary mixtures (where the word “organic” is used here to mean non-ionic organic liquids; Table 3). Even ternary mixtures such as IL/ethanol/water, can be phase-split by the application of CO_2 gas. Ionic liquid/organic pairs are

Table 3. Minimum Pressures of CO_2 Required To Cause the Formation of Two Liquid Phases from a Mixture of Two Miscible Liquids at 40 °C^a

solvent A	solvent B	<i>P</i> , bar	ref
water	methanol	80	139
water	1-propanol	68	138
water	2-propanol	78	140
water	acetone	26	145
water	acetic acid	75, 78	146, 147
water	propanoic acid	72, 78	147, 148
water	butanoic acid	40	147
water	THF	<10	149
water	1,4-dioxane	<28	150
water	MeCN	<19	150
water	MeCN	25 ^b	151
[bmim]PF ₆	water	30 ^c	144
[bmim]PF ₆	methanol	69	142, 143, 152
[bmim]PF ₆	MeCN	77	143
[bmim]NTf ₂	methanol	80	143
[bmim]NTf ₂	MeCN	74	143

^a See the original reference for the composition of the original binary mixture of liquids. ^b Using ethylene as the expanding gas at 70 °C. ^c At 20 °C.

a special case because the IL has essentially no solubility in the CO_2 gas. As a result, the UCSP is the same as the pressure that would be required to dissolve the “organic” liquid into CO_2 in the absence of an IL.¹⁴³

Other gases, such as C_2H_4 , C_2H_6 , and N_2O are capable of triggering immiscibility in pairs of liquids.¹⁵³ The first observation of the effect, by Elgin and Weinstock, was with ethylene.¹⁵⁴ A similar effect using liquid CO_2 was described for many systems by Francis.³² The gas used to trigger immiscibility needs to be compressible; N_2 , for example, behaves as an incompressible ideal gas (because its T_c is too far below ambient temperature), and therefore it does not trigger immiscibility, at least in the one system tested.¹⁴³

Triggering of immiscibility is used as a means of separating liquid components in the method called Gas Anti-Solvent Fractionation, as illustrated by Catchpole¹⁵⁵ for the example of separating triglyceride oil from hexane by the application of CO_2 and by the Brennecke group¹⁴² for the separation of the ionic liquid [bmim]PF₆ from methanol.

A solute dissolved in water/alcohol mixtures will partition between the two liquid phases when immiscibility is triggered. The partitioning is a strong function of the CO_2 pressure and the temperature.^{141,156–159} The mole fraction partition coefficient (ratio of the mole fractions of the solute in the two liquid phases, $K = X_{L1}/X_{L2}$) for the solute must necessarily be 1 at the pressure when the liquid-phase first separates into two, but then deviates from 1 as the CO_2 pressure is increased.

While the above examples all illustrate the use of CO_2 or similar gases to trigger immiscibility in a mixture of two miscible liquids, it is also possible to do the reverse. That is, it is possible to trigger miscibility in mixtures of two immiscible liquids. For example, two liquids that are immiscible with each other because they differ in fluorophilicity (one is fluorophilic and the other is fluorophobic) may form a single liquid phase upon expansion with CO_2 . The term “fluorophilic” means able to dissolve highly fluorinated organic compounds such as perfluoroalkanes. Carbon dioxide is inherently fluorophilic, for reasons that are not entirely understood. Many organic solvents, including toluene, methanol, and acetone, are fluorophobic but become fluorophilic upon expansion with CO_2 . Thus, CO_2 expansion

Table 4. Pressures of CO₂ (bar) Required to Induce Miscibility in Organic/Fluorous Liquid Mixtures at 25 °C¹⁶⁰

organic solvent	perfluorohexane	FC-75 ^a
THF	19.2	19.2
cyclohexane	26.4	26.9
acetic acid	27.6	na
toluene	32.3	33.5
acetonitrile	40.0	40.2
methanol	45.9	47.4
decalin	53.9	57.7

^a Perfluoro-2-butyltetrahydrofuran.

of a binary mixture of a fluorophobic organic solvent with a fluorous (highly fluorinated) solvent will trigger miscibility. The pressure of CO₂ required to make organic/fluorous liquid pairs become miscible has been measured (Table 4).¹⁶⁰ The pressure required depends on the interactions between the organic and CO₂ and between the organic and the fluorous solvent. The miscibility pressure is lowest for those organic solvents (such as THF) that inherently have greater miscibility with fluorous solvents and those in which CO₂ is highly soluble.^{160,161}

Applications of induced miscibility or immiscibility to catalysis and catalyst recovery are described in sections 3.5 and 3.9.

Expansion of mixtures of perfluoropolyether oil, water, and a surfactant by CO₂ has been shown to trigger the formation of microemulsions.¹⁶² The surfactant was [Cl{CF₂CF(CF₃)O}_nCF₂CO₂]⁻NH₄⁺ (*n* ≈ 3). The mixture composition was typically 5 wt % surfactant in the oil, with a 20:1 water/surfactant mole ratio. Microemulsion formation was observed at CO₂ mole fractions of 70% and above. Absorption spectra of methyl orange dye dissolved into the micelles showed that the micelle cores are aqueous and acidic.

2.6. Modeling

2.6.1. Simulation of Compressible Gas Solubility in Liquid Solvents

The VLE data for CXLs are not always available in the literature. Empirical equations of state (EoS) have been used to estimate the VLE of various fluids or fluid mixtures under high pressures,^{163,164} among which the Peng–Robinson (PR-EoS) is most frequently used for simulating CO₂ + organic systems.^{165,166} Although PR-EoS has proven effective in predicting many CO₂ + organic systems, it fails to describe some complicated systems, that is, those that contain two immiscible liquid phases.²⁴

To obtain a detailed molecular-level understanding of the phase behavior, transport properties, and solute (reactant and catalyst) solubilities in the continuum of the CO₂-expanded solvent (CXL) system, molecular modeling is useful. Recent advances in computing power and algorithms combined with the availability of force fields have enabled the calculation of high-pressure VLE with molecular simulation methods. The reported methods include Gibbs Ensemble Monte Carlo (GEMC),^{167,168} histogram-reweighing,^{169–171} and Gibbs–Duhem integration.¹⁷²

Laird's group³⁷ examined the structure and phase equilibria for several CO₂ + organic binary systems using the GEMC molecular simulation method. The organic liquids studied include acetonitrile, methanol, ethanol, acetone, acetic acid, toluene, and 1-octene. Molecular interaction parameters were obtained by fitting the model first with the reported

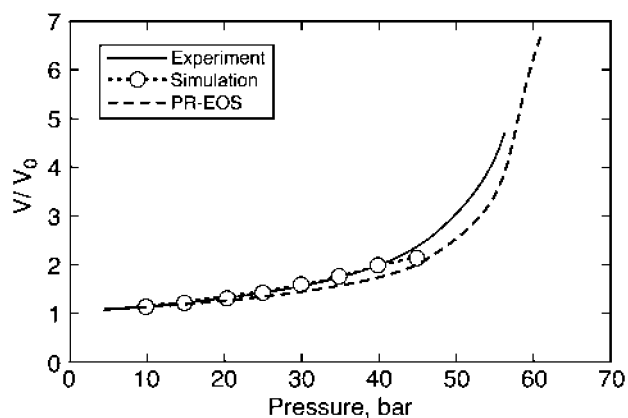


Figure 14. Molecular simulations for acetone expansion by CO₂ at 30 °C.³⁷ (Reprinted with permission from ref 37. Copyright 2006 American Chemical Society).

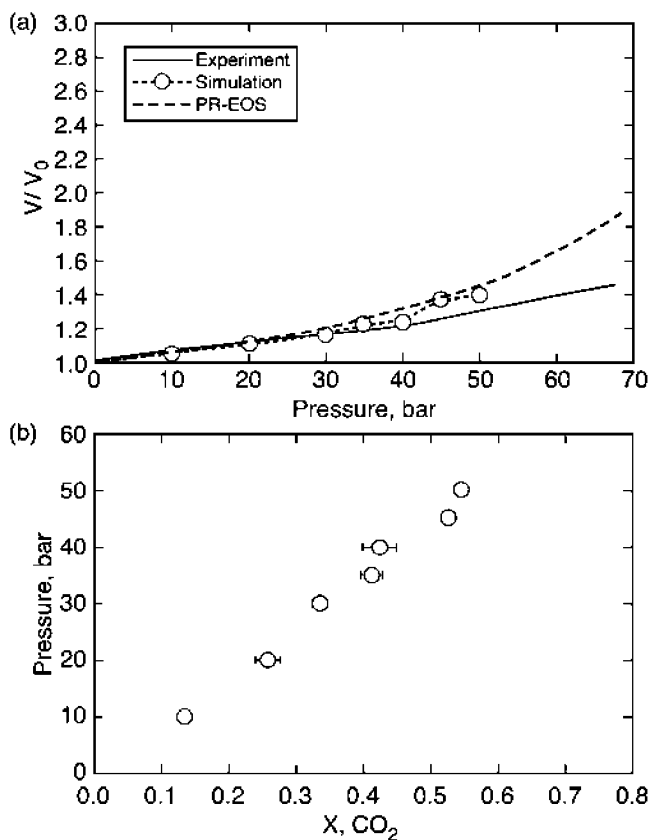


Figure 15. Molecular simulations for 1-octene expansion by CO₂ (a) and the equilibrium liquid-phase composition of CO₂ (b) at 60 °C.³⁷ (Reprinted with permission from ref 37. Copyright 2006 American Chemical Society).

experimental data for pure components. The model was able to accurately reproduce the experimental data. In all cases, the molecular simulation results were found to be as good as, and in many cases superior to, the predictions by PR-EoS.

Figures 14 and 15 present the expansions of acetone by CO₂ at 30 °C and 1-octene at 60 °C. Simulation results by PR-EoS are also included. The simulated values from the Monte Carlo method and PR-EoS agreed well with each other and with the experimental data for acetone expansions. The molecular models, unlike empirical models, also provide insights into fundamental interactions that occur in the solvent matrix. As inferred from Figure 15b for the CO₂ + 1-octene binary system, a significant amount of CO₂ (~50

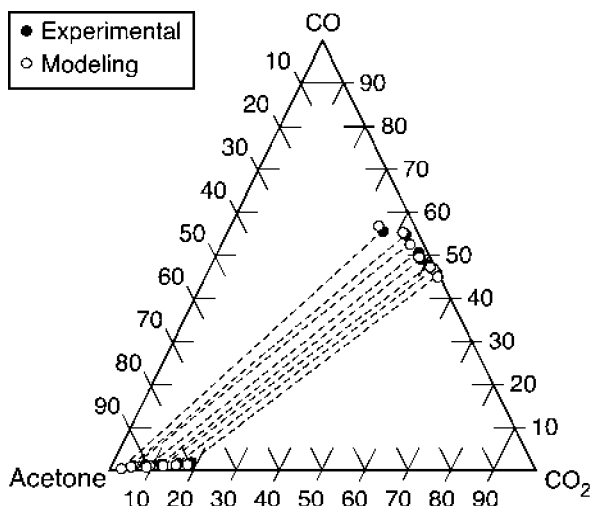


Figure 16. Comparison of experimental and predicted CO₂/CO/acetone vapor/liquid equilibrium.³⁸ Axes indicate mole %.

mol %) is dissolved in 1-octene even at very mild pressures (less than 5 MPa), confirming the potential of dense CO₂ to significantly replace conventional solvents at relatively mild pressures. As discussed in sections 2.3 and 2.6.3, Hernandez' group⁴⁷ and Maroncelli's group⁴⁹ have also modeled GXLS using molecular simulation techniques.

For class III GXLS involving ILs, Shiflett and Yokozeki⁸⁹ used a simple EoS to accurately predict the phase behavior of CO₂ and IL mixtures. The Henry's law constants and the volume change of solutions are also predicted well with the EoS model. In a subsequent study, Shiflett and Yokozeki⁹⁰ successfully correlated the solubilities of several hydrofluorocarbons in [bmim][PF₆] and [bmim][BF₄] in well-known solution models (Margules, Wilson, and NRTL activity coefficient equations). McGinn's group^{51,173} employed molecular simulation methods to compute Henry's constants of water, carbon dioxide, ethane, ethene, methane, oxygen, and nitrogen in [bmim][PF₆]. While the simulations predict higher solubilities than reported experimental values for most of the gases, they nevertheless provide valuable insights into the interactions responsible for the experimentally observed solubility trends.

2.6.2. Simulation of Permanent Gas Solubility in Expanded Liquids

The PR-EoS, using only binary interaction parameters fit to binary data, is successful in predicting the phase behavior of the ternary systems involving gas, CO₂, and acetone.¹³⁶ Excellent agreement is noted between experimental and predicted VLE data for O₂ + CO₂ + solvent and CO + CO₂ + solvent ternary systems where the solvent is either acetonitrile or methanol. Figure 16 shows a ternary diagram for the CO₂/CO/acetone system at 30 °C with several tie lines that connect the equilibrium composition in the CO₂-expanded liquid phase (the lower points that lie along the acetone/CO₂ axis) and in the gas phase (the top points that lie along the CO₂/CO axis). A relatively large two-phase region exists. The experimental tie lines are predicted remarkably well by the PR-EoS employing only binary interaction coefficients of CO + CO₂ (0.17),¹³⁰ CO + acetone (0.11 [fitted with experimental data]), and CO₂ + acetone (0.0128)¹⁷⁴ in the mixing rules. The good fit between the experimental data and simulated results is attributed to the fact that the CXL phase (along the acetone/CO₂ axis) is lean

in CO and the gas phase is lean in acetone, and these two phases may thus be approximated as pseudobinary systems.

2.6.3. Transport Properties

Using the measured diffusion coefficients of benzene in CO₂-expanded methanol, Eckert's group employed the modified Stokes–Einstein equation¹⁷⁵ to estimate the viscosity of each mixture.⁸⁷ The predicted values at 50 °C and 150 bar showed a nearly linear viscosity variation between the pure component values, with the viscosity of CO₂-expanded methanol decreasing with increasing CO₂ content. Kho et al.⁸⁸ successfully modeled the viscosity reduction in CO₂-expanded fluorinated solvents using the method of Orbey and Sandler.

Laird's group has estimated the translational and rotational diffusion constants of pure MeCN and CO₂ using the existing potentials and MD simulation.⁴⁸ The translational diffusion coefficients and molecular reorientation times for pure MeCN and CO₂ are seen to differ by only a few percent from experimental values at 25 and 75 °C. In the mixture, there is a strong trend toward increasing MeCN translational diffusion as the CO₂ mole fraction in the CXL increases. The opposite trend is seen for rotational diffusion constants. Maroncelli's group⁴⁹ employed molecular dynamics simulations of CO₂-expanded cyclohexane, acetonitrile, and methanol to simulate viscosities and diffusion coefficients. On the basis of comparisons to the limited experimental data available, they conclude that simple intermolecular potential models previously developed for the pure components provide reasonable representations for the dynamics of the CXLs. Hernandez's group⁴⁷ employed molecular dynamics simulation to compute self-diffusion coefficients of methanol in CO₂-expanded methanol and of acetone in CO₂-expanded acetone. Although the computed values for diffusion coefficients are not in exact agreement with experimental values, the models nevertheless reproduce the general trend of enhanced solvent diffusivity with CO₂ addition.

For class III GXLS, models for the lowering of the T_g of polymer melts by CO₂ dissolution and the concomitant viscosity reduction have been modeled. For polymer melts containing dissolved gases (class III solvents), the viscosity curves (shear viscosity η vs shear rate $\dot{\gamma}$) obtained at different CO₂ concentrations can be shifted to the curve obtained for pure polymer using a concentration-dependent shift factor

$$a_c = \eta_0 / \eta_{0,P}$$

where η_0 is the shear viscosity of a polymer melt containing dissolved gas, and $\eta_{0,P}$ is the shear viscosity of the pure polymer. Such a normalized curve generated for PDMS/CO₂ solution at 50 °C is shown in Figure 17.¹⁷⁶ To consider the cumulative effects of the temperature, pressure, and concentration, the respective shift factors are multiplied together ($a_T a_c a_p$) to generate the master curve. It is generally believed that two mechanisms contribute to the viscosity reduction in polymers upon CO₂ addition. The first is the dilution of chain entanglements in the melt upon gas dissolution. The second and more predominant mechanism involves generation of additional free volume, which increases chain mobility. Doolittle's free volume theory¹⁷⁷ correlates viscosity and free volume.

Gerhardt et al.¹⁷⁶ and Kwag et al.¹⁷⁸ used Doolittle's free volume theory to successfully predict shift factors for PDMS/CO₂ and PS/CO₂ systems. Modified versions of the free

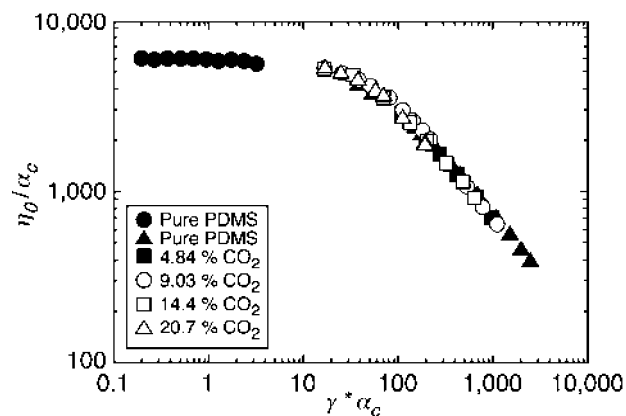


Figure 17. The master viscosity curve (based on the concentration of CO₂) for the PDMS–CO₂ solution at 50 °C.¹⁷⁶ (Reprinted with permission from ref 176. Copyright 1998 Wiley Periodicals, Inc.).

volume theory was used by other researchers^{103,108,110} to reliably predict the melting point depression of various other polymers due to dissolved CO₂ and the resulting enhancement in the free volume of the polymer.

Morgan et al.⁹¹ measured diffusivities of carbon dioxide, ethylene, propylene, 1-butene, and 1,3-butadiene in five imidazolium-based ILs and one phosphonium-based IL at 30 °C covering a liquid viscosity range of 10–1000 cP. The experimental diffusivity data were correlated in terms of the gas molar volume, the IL viscosity, and density. As discussed earlier (section 2.4.3), Shiflett and Yokozeki⁸⁹ have also correlated measured diffusion coefficients in ILs.

2.6.4. Macroscopic Models of Mixing and Reactors

In many applications of GXLs, the mixing of the compressed gas and the liquid is a critical step. For example, during batch gas antisolvent (GAS) recrystallization (described in section 3.1.2), the addition rate of CO₂ to a liquid solution determines the rate of supersaturation buildup in solution, which ultimately controls the particle formation process. Mazzotti's and Subramaniam's groups¹⁷⁹ investigated the effects of mass-transfer resistance on volume expansion, both theoretically by development of a mathematical model of the mass-transfer phenomena under typical GAS recrystallization conditions and experimentally through volume expansion experiments (CO₂ in toluene). The detailed model included correlations based on dimensionless groups to predict the volumetric mass-transfer coefficient. The model parameters appearing in the correlations for the mass-transfer coefficient were estimated by fitting the experimental results. The role of operating parameters such as the stirring rate and aeration mode was assessed using the model. As shown in Figure 18, satisfactory agreement between model results and experimental data was found in all cases. Such models are clearly essential for the rational interpretation of the dependence of operating parameters on particle size and morphology. Fusaro et al.,¹⁸⁰ comparing the GAS and PCA (Precipitation with Compressed Antisolvent) processes, showed that the 2 orders of magnitude disparity in the average particle size is mirrored by a similar disparity in the characteristic *mass transfer times* for the two processes. These results suggest that PCA and GAS, with common underlying mass transfer mechanisms, may be essentially viewed in a continuum of characteristic mass transfer time scales with the higher *mass transfer time constants* yielding progressively larger particles.

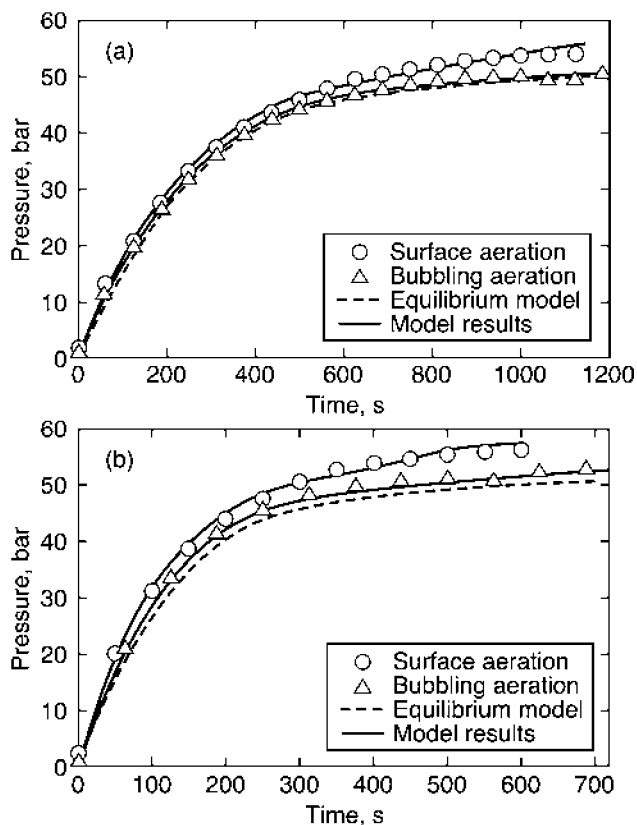


Figure 18. Evolution of pressure in batch mixer under different aeration modes during liquid pressurization with gas. Operating conditions: $T = 20$ °C, $N = 300$ rpm, (a) $Q_{\text{CO}_2}/V_\alpha = 0.200$ min⁻¹; (b) $Q_{\text{CO}_2}/V_\alpha = 0.400$ min⁻¹. (Q_{CO_2} = CO₂ addition rate; V_α = initial volume of liquid phase)¹⁷⁹ (Reprinted with permission from ref 179. Copyright 2003 American Chemical Society).

Guha et al.¹⁸¹ investigated the effects of syngas mass transfer limitations on the catalytic hydroformylation of 1-octene through a mathematical model and experimental studies using a high-pressure ReactIR apparatus. A comprehensive mathematical model that incorporates mass transfer rates, kinetic parameters, and phase equilibrium was developed for the catalytic hydroformylation of olefins. The model predicted that syngas mass transfer limitations could cause the induction period observed during the experimental studies in CXLs.¹⁸² Follow-up experimental studies in a ReactIR confirmed that the induction periods are indeed reduced several fold through increased agitation to improve mass transfer rates.

3. Applications

3.1. Particle Formation

A variety of methods for the preparation of fine, and preferably monodisperse, powders from organic, inorganic, or organometallic solids have been developed based upon the phase behavior of CXL (Figure 19).^{183–185} The organic particles have applications in pigments,¹⁸⁶ foodstuffs,¹⁸⁷ explosives,¹⁸⁸ and pharmaceutical compounds.^{184,189,190} The processes involve either precipitation from solutions or melting of the compound followed by freezing. Expansion of the solution or the neat compound by CO₂ is used in many such processes, as explained below. Particles, once formed, can also be dried or fractionated with the help of CO₂.

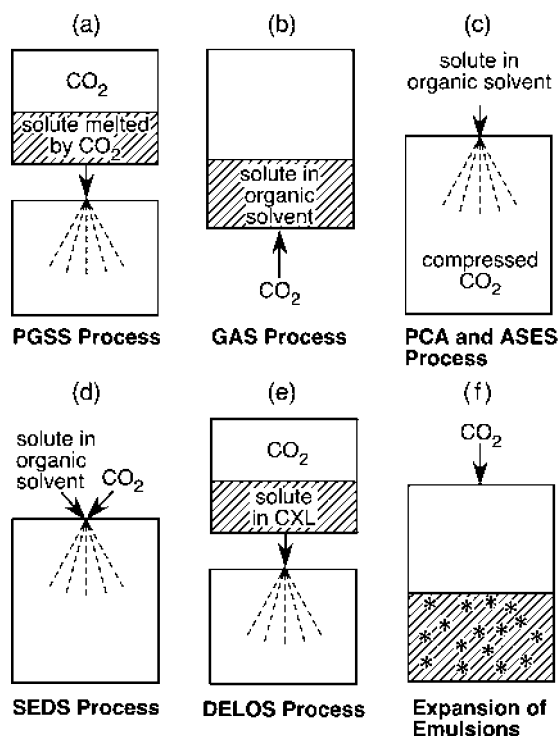


Figure 19. Several processes for the preparation of particles.

3.1.1. Particles from Gas-Saturated Solution (PGSS)

Melting a solid by CO₂ expansion and then forcing the melt through a small nozzle, so that it simultaneously sprays and degasses, causes the rapid depressurization and cooling of the melt; the result is a fine powder precipitate (Figure 19a). This technique, called PGSS (Particles from Gas-Saturated Solution), only works at temperatures close to the T_m of the compound. For example, Sencar-Bozic et al. found that Nifedipine, a calcium-channel blocker (T_m 172–174 °C),¹⁹¹ after processing by PGSS at 185 °C, had a smaller particle size and much more rapid rate of dissolution in water than the unprocessed material,¹⁹² although the temperature required for the process was too high to be practical for many pharmaceuticals. Even Nifedipine showed some degradation during the micronization. To make the PGSS usable at lower temperatures, the researchers evaluated the micronization of a mixture of poly(ethylene glycol) (PEG, MW 4000) with Nifedipine at 50 °C. Finely powdered coprecipitate was obtained, without observable degradation.

The PLUSS process (Polymer Liquefaction Using Supercritical Solvation) similarly uses dissolution of CO₂ into a polymer to cause it to swell or melt. An active ingredient is then mixed in. Releasing this mixture through a nozzle produces finely powdered microcapsules. Shine and Gelb¹⁹³ described in their patent an example of encapsulating a vaccine into particles of polycaprolactone.

3.1.2. Gas Antisolvent (GAS)

There are several particle formation processes that rely on CO₂-expansion of a solution to trigger precipitation. The CO₂ is therefore serving as an antisolvent. The simplest of these processes is GAS (Gas Anti-Solvent), in which CO₂ is introduced into a chamber already containing a solution of the solute in an organic solvent. Expansion of the solvent lowers the solubility of the solute to such an extent that the solute precipitates. Afterward, the vessel contents are passed out of the vessel and the solids separated from the expanded

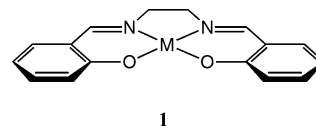
liquid (Figure 19b).¹⁸³ The method was first described by Krukonis and Gallagher.¹⁹⁴

3.1.3. Precipitation with Compressed Antisolvent (PCA) and Aerosol Solvent Extraction System (ASES)

The PCA (Precipitation with Compressed Antisolvent) process is simply the reverse of the GAS process. The solution of solute in organic solvent is sprayed into a chamber that already contains pressurized CO₂ (Figure 19c). Expansion of the solvent droplets happens rapidly, forcing precipitation of the solute in the form of much finer particles than observed with GAS. Afterward, the organic solvent is washed away from the particles with fresh CO₂.¹⁸³ PCA can also be used to prepare crystals that incorporate CO₂ molecules (or molecules of another compressible gas) into the crystal structure of the precipitated material.^{195,196}

In the ASES (Aerosol Solvent Extraction System) variation of this process, the solvent is not only expanded but is in fact completely dissolved into the *sc*CO₂. This process can also be performed with the CO₂ flowing through the vessel, concurrently or countercurrently with respect to the organic solution, so as to extract and remove the organic solvent from the chamber.¹⁹⁷

While a majority of PCA/ASES studies have concerned the preparation of particles of organic compounds, there are a few exceptions. Hutchings et al.¹⁹⁸ prepared a solution of vanadium phosphates in isopropanol by the reaction of H₃-PO₄ and VOCl₃ and then precipitated the product by PCA. The amorphous solid was an active catalyst for the oxidation of butane to maleic anhydride. Johnson et al.¹⁹⁹ prepared metal complexes containing salen ligands (structure 1) and then produced rod-shaped particles of lengths of 700 nm by PCA of CH₂Cl₂-solutions of the complexes. The particles have potential applications in capture of gases or as heterogeneous catalysts.



1

3.1.4. Solution-Enhanced Dispersion by Supercritical Fluids (SEDS)

Simultaneous feed of supercritical CO₂ and a solution of solute in an organic solvent into a coaxial nozzle (Figure 19d) produces finer particles than in the conventional PCA or ASES processes. This variation, called SEDS (Solution-Enhanced Dispersion by Supercritical fluids), was developed by Hanna and York.²⁰⁰

Subramaniam's group developed a process that employs an ultrasonic nozzle and *sc*CO₂ as the energizing medium to form fine droplets of drug solution. The *sc*CO₂ also selectively extracts the solvent from the droplets, precipitating the drug. Submicron particles of hydrocortisone, ibuprofen, insulin, and paclitaxel were formed using this technique.^{201–203}

3.1.5. Depressurization of an Expanded Liquid Organic Solution (DELOS)

In the DELOS (Depressurization of an Expanded Liquid Organic Solution) technique, a solute is dissolved in an organic solvent and the solution expanded. The concentration of the solute is sufficiently low that the expansion does not trigger precipitation. However, the pressure is then suddenly lowered, causing the dissolved CO₂ to rapidly come out of

solution. The resulting temperature drop is dramatic and sufficient to induce precipitation of the solute as a fine powder (Figure 19e).^{204,205} The same effect but with lower operating pressures is possible if one uses 1,1,1,2-tetrafluoroethane instead of CO₂.²⁰⁶

3.1.6. Precipitation of Particles from Reverse Emulsions

Compounds dissolved in the aqueous core of reverse emulsions can be precipitated as solid particles by the expansion of the emulsion with CO₂ (Figure 19f). The technique has been demonstrated for a protein²⁰⁷ and an enzyme.²⁰⁸ For example, the protein trypsin has been precipitated as fine particles of average diameter 10 nm from reverse emulsions by expansion with CO₂ (50 bar, 20 °C).²⁰⁷ The emulsion before expansion consisted of decane continuous phase with 100 mM surfactant, water (water/surfactant mole ratio $w_0 = 20$), and trypsin protein (0.5–0.8 mg/mL).

Inorganic particles can be prepared and precipitated by a related procedure.^{209,210} For example, Zhang et al.²⁰⁹ showed that mixing two reverse emulsions, one containing ZnSO₄ dissolved in the aqueous cores and the other Na₂S (both in AOT-stabilized water in iso-octane emulsions), causes the formation of ZnS particles in the combined emulsion. The particles are collected by expansion of the emulsion with CO₂.

3.1.7. Particle Processing

Particles dispersed in a solvent can be fractionated by gradual expansion of the solvent. Roberts' group^{211,212} has described the use of gradually increasing pressures of CO₂ to cause the precipitation of gradually decreasing particle size fractions of particles. The particles were gold or silver nanoparticles protected by alkanethiols. To prevent later fractions from precipitating onto fractions that had already precipitated, they used an Archimedes screw inside the high-pressure vessel to move the remaining suspension after each fraction precipitates.

Nanoparticle thin films have a variety of potential applications if they can be obtained in evenly distributed close-packed monolayers on a surface. However, attempts to obtain such an even monolayer from a suspension of particles by evaporation of the solvent can result in a very uneven distribution with some areas containing high concentrations and other areas being entirely devoid of particles. The fault lies with the high interfacial tension and capillary forces that exist during the removal of the solvent. Roberts' group has shown that expansion of the solvent by CO₂, followed by raising the temperature to 40 °C and flushing with fresh CO₂, allows the precipitation of the particles and complete removal of the solvent without disruption of the even monolayer.^{213,214}

Subramaniam's group employed the PCA process for particle coating.^{201,215} Here, *sc*CO₂ is used to fluidize the core substrate particles. The *sc*CO₂ also removes the solvent from the coating solution sprayed on the substrates, thereby precipitating the coating. Glass and non-pareil sugar beads (1–2 mm) were coated with a thin layer of RG503H polymer, either as a deposit of fine particles or as a continuous film. The CO₂-based coating process expands the range of substrate/solvent combinations possible with the conventional air-suspension Wurster coater, making it feasible to coat water-soluble substrates with solutes sprayed from organic solvents.

3.2. Enhanced Oil Recovery

Pumping of crude oil out of natural reservoirs only recovers a fraction of the available oil. Enhanced oil recovery (EOR)²¹⁶ is a process by which a significant part of the crude oil remaining in the reservoir can be flushed out. Typically, water, CO₂, or both are injected into an injection well and displace the remaining oil toward the production well. The CO₂ pressure and temperature are fixed by the conditions in the reservoir.²¹⁷ The use of CO₂ offers several advantages: it lowers the viscosity of the oil by expansion, permeates rock pores better than water, helps to selectively move the lighter components of oil, and can be left inside the reservoir as part of a strategy for greenhouse gas mitigation. The choice of method depends on the motivation for using CO₂, either a desire to maximize oil production (by CO₂ utilization) or a desire to maximize the amount of CO₂ left underground (i.e., CO₂ storage), although it is possible to co-optimize methods to achieve both objectives.²¹⁸

Dissolution of CO₂ in crude oil does not lead to a large volumetric expansion but does contribute to a significant reduction in viscosity.^{219–221} For example, Ada crude (a heavy crude oil)²¹⁹ expands by only 20% at 21 °C and 69 bar CO₂, suggesting that crude oil is a class III-expanded solvent rather than class II. The reason for the failure of crude oil to expand greatly is the poor solubility of CO₂ in crude (see Figure 1 in section 2.1). Nevertheless, the expansion results in a drop in viscosity^{219,222} which is believed to contribute greatly to the effectiveness of CO₂ as an EOR injection fluid. The viscosity of Ada heavy crude drops from 400 to 22 cp upon expansion with 69 bar of CO₂. Other gases have the same effect but to differing degrees.^{220,221} Propane is more effective than CO₂, while methane and especially N₂ are less effective. Hydrostatic pressure causes a rise in the viscosity.

Enhanced oil recovery using CO₂ expansion of crude is not without problems. Expansion of crude by CO₂ also has the effect of decreasing the solubility of asphaltene fractions, with the result that they may precipitate inside the reservoir.^{217,223,224} The acidity that results from the combination of CO₂ and natural or added water leads to the dissolution or loosening of some carbonate minerals and clays,²²⁴ which may then be deposited elsewhere and thereby restrict flow. Nevertheless, enhanced oil recovery using CO₂ expansion is the largest scale application, by far, of gas-expanded liquids.

3.3. Polymer Processing

Processing of polymers often requires temperatures above the T_m or T_g of the polymer, which can be energetically expensive and, if thermally sensitive polymers or other species are involved, damaging to the materials. As described in section 2.4.2, CO₂ dissolution into an organic compound lowers its T_m . For polymers, CO₂ dissolution has been shown to lower the melting temperature,^{66–72} the crystallization temperature,^{67,69,83} and the glass transition temperature^{93,94,96} and to raise the rate and degree of crystallization^{71,84} for a variety of polymers including *t*-butyl poly(ether ether ketone),²²⁵ ethylcellulose,²²⁶ methyl poly(ether ether ketone),⁸⁵ poly(bisphenol A carbonate),^{69,97,227,228} polycaprolactone,⁷² poly(ether ether ketone),²²⁹ poly(ethylene glycol)/poly(ethylene oxide),^{68,71,82} poly(ethylene terephthalate),^{66,84,230} poly(methyl methacrylate),^{93,95,96} poly(*p*-phenylene sulfide),²³¹ polypropylene,^{67,83} polystyrene,^{93,96,97,232,233} poly(vinyl chlo-

ride),⁹⁷ poly(vinylidene fluoride),^{70,234} and polyvinylpyrrolidone.²²⁶

Polymer processing methods that take advantage of the melting-point lowering and viscosity-lowering effects of dissolved CO₂ have been used to adjust particle size¹⁸⁵ and morphology^{71,72,235,236} of polymers and to facilitate extrusion,²³⁷ foaming,²³⁸ impregnation,¹⁸⁵ and mixing or co-molding of polymers.²³⁹ With thermally sensitive polymers, CO₂ allows the polymer processing temperature to be lowered, thereby avoiding polymer decomposition, cyclization, or cross-linking. For example, acrylonitrile copolymers, which have an unfortunate tendency to cross-link, can be processed at low temperatures and without the use of added solvents if CO₂ is used to lower both the T_g and the viscosity of the melt.²⁴⁰ At a loading of 6.7 wt % CO₂, a 31°C reduction in the T_g of Barex (an acrylonitrile copolymer) and a roughly 3-fold reduction in viscosity was obtained, allowing a 30 °C lowering of the processing temperature, with the only downside being the requirement for 172 bar of CO₂ pressure. This type of CO₂-induced plasticization for processing can be combined with the foaming effect of CO₂ when it is released from the polymer melt. The result is then a high-surface area, porous extruded polymer.²²⁶

Impregnation of active ingredients into polymers is particularly important for pharmaceutical applications. Mandel and co-workers showed that one could soften a polymer with CO₂ pressure enough to allow the polymer to be mixed at mild temperatures with heat-sensitive species such as an enzyme.^{241,242} The mixing of polymers with active pharmaceutical ingredients can be performed in combination with particle formation using PGSS or any of the other technique described in section 3.1.¹⁸⁵

The field of polymer processing using CO₂-induced lowering of T_m and T_g has been extensively reviewed.^{100,101,242,243}

3.4. Separations and Crystallizations

In traditional crystallization, supersaturation to induce nucleation and crystal growth is achieved by cooling. To achieve uniform cooling, temperature gradients have to be avoided, which is a practical challenge. In contrast, mixing a compressed gas uniformly in a liquid solution may be more easily achieved. In the GAS process (described in section 3.1.2), supersaturation and nucleation occur uniformly throughout the solution yielding submicron to micron size particles in a narrow size distribution. Pharmaceutical applications have received the most attention due to the potential of the GAS-produced particles for enhancing the dissolution rates of sparingly water-soluble drug molecules and in controlled-release formulations.

Growth of large crystals, which are useful for crystallographic studies, must take place more slowly than the kind of crystallization used to generate fine powders. Techniques based upon CO₂ expansion of solvents can still be used, as long as they are modified to allow slow crystal growth. For example, dissolving a fluororous compound in a CO₂-expanded solvent and then slowly releasing the CO₂ pressure results in a supersaturated solution from which the compound slowly crystallizes.^{244,245}

The tunability of GXLs has also been exploited to purify compounds and to effect separation of mixed solutes in solution. For example, GAS recrystallization with CO₂ was used to separate citric acid from oxalic acid²⁴⁶ and to isolate and purify β -carotene from a mixture of carotene oxidation

products.²⁴⁷ It should be noted that mixtures of CO₂ and organic solvents (termed “enhanced fluidity liquids” that possess better transport properties than the neat solvents) have also been used as HPLC mobile phases^{20,248,249} to perform separations. Applications include reversed-phase HPLC,^{250–252} size-exclusion chromatography,^{21,253–256} and chiral separations.^{257,258}

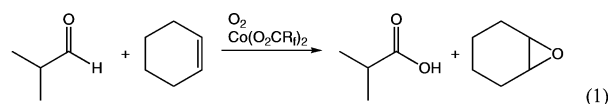
3.5. Postreaction Separations

Homogeneous catalysis is associated with many industrially significant processes such as hydrogenation, Wacker-Hoechst oxidation, C–C linkage of olefins, syngas-based reactions, functionalizations (hydrocyanation and hydro-silylation), isomerization, and metatheses. Homogeneous catalysts possess many advantages over heterogeneous catalysts such as superior activity with high metal efficiency and higher selectivities (stereo-, regio-, and chemoselectivities). A main goal in homogeneous catalysis research is efficient recovery and recycling of the catalyst complex. In catalysis involving expensive metals or ligands, catalyst separation and recycling is often the key to economic viability.

Postreaction catalyst separation schemes often involve the use of solvents to effect polarity switches in the liquid-phase reaction media to separate the reactants, products and catalysts. The use of compressed gases such as CO₂ offers a convenient and environmentally beneficial method to tune the polarity of the reaction medium. Indeed, many groups have exploited this to demonstrate promising catalyst separation schemes. The Busch/Subramaniam team exploited GXLs for separating oxidation catalysts postreaction.⁴⁴ Isothermal CO₂ addition to a solution of CH₃CN containing a known amount of the dissolved catalyst, [$\{N,N'$ -bis(3,5-di-*tert*-butylsalicylidene)1,2-cyclohexanediiimino(2-)}cobalt(II)]₂, that is, Co(salen*), caused the catalyst to precipitate when roughly 80 vol % of the organic solvent is replaced by compressed CO₂ at 50 °C. It is noteworthy that the total pressures for precipitation are on the order of only tens of bars. In contrast, pressures exceeding 100 bar are required for solubilizing the catalyst in *sc*CO₂; for example, 207 bar at 70 °C for Co(salen*).²⁵⁹ As explained in section 2.5.1, the Subramaniam group has successfully used CO₂ addition postreaction to demonstrate the concept of precipitating Rh complexes at relatively mild pressures and temperatures.¹²⁸ These results suggest new opportunities for catalyst ligand design to permit facile and complete catalyst recovery with GXLs.

In fluororous biphasic systems, a homogeneous catalyst is modified with fluorinated ligands such that the catalyst is preferentially soluble in the fluororous phase. The immiscibility of the fluororous and organic phases is exploited to effect the separation of reactants and catalysts. Often, high temperatures or other additives such as benzotrifluoride are used to induce miscibility and eliminate phase transfer resistances. The Eckert/Liotta group¹⁶⁰ has demonstrated the addition of compressed CO₂ to fluororous biphasic chemical systems to effect postreaction separations. Following the homogeneous reaction, depressurization induces a phase split, with the catalyst remaining in the fluororous phase and the product in the organic phase. This CO₂ “miscibility switch” was demonstrated for two model reactions. The hydrogenation of allyl alcohol using a Pd nanoparticle catalyst in a fluororous dendrimer was performed in biphasic (CO₂ absent) or monophasic (55 bar CO₂) mixtures of perfluorotributylamine

and allyl alcohol. The monophasic conditions gave 70% greater rates of hydrogenation. After the monophasic reaction, the CO₂ pressure was released so that the liquid-phase would split into the fluoruous and organic phases, facilitating separation of the product from the catalyst.¹⁶⁰ A similar rate increase²⁶⁰ and facilitated product/catalyst separation were observed for a homogeneously catalyzed olefin epoxidation (eq 1, R_f = perfluoropolyether).



In another application, the Eckert/Liotta group employed either liquid or compressed gas (CO₂) addition to mixed organic-aqueous tunable solvents (OATS) to facilitate phase separation and recycle enzymes.¹⁴⁹ When OATS is used, reactions between water-soluble catalysts and moderately hydrophobic substrates can be run homogeneously. For example, the dimethyl ether (DME)–water system has been employed for alcohol dehydrogenase-catalyzed reduction of hydrophobic ketones. Following reaction, the DME-rich phase, containing the product, is separated from the aqueous phase by depressurization and vaporization to recover DME. The enzyme is retained in the aqueous phase, which is recycled.

The Jessop and Eckert/Liotta groups together reported a system for using CO₂ expansion of a solvent to shuttle a catalyst from a solid phase to solution phase and back again. In this method, a fluoruous silica support, impregnated with a fluoruous homogeneous catalyst, is placed into a fluorophobic liquid solvent along with reactants and reagents required for the reaction. The solvent is then expanded with CO₂ to cause it to become fluorophilic and able to extract the fluoruous catalyst out of its support. The catalyst then promotes the solution-phase reaction in a homogeneous manner. When the reaction is complete, the CO₂ pressure is released to return the solvent to its normal fluorophobic condition and thereby to send the catalyst back into its support. The method was demonstrated using hydrogenation of styrene using a fluoruous version of Wilkinson's catalyst as a test reaction. Catalyst precursor, styrene, cyclohexane, and fluoruous silica were placed in a vessel at 40 °C (top left of Figure 20). H₂ and CO₂ (60 bar) were added, at which point the solvent expanded and the catalyst became soluble. After the reaction, the gases were vented, causing the catalyst to leave the solution and become entrapped by the fluoruous silica. The liquid product could be decanted, and the fluoruous silica/catalyst solid phase was re-used repeatedly. Rh losses to the liquid product were too low to be detectable by ICP/AA.²⁶¹

3.6. Switchable Solvents

A switchable solvent is a solvent that can be reversibly converted from one form to another, where the two forms differ in one or more physical properties. For example, the solvent might be fairly polar in one form but much less polar in the other. Very few switchable solvents have been identified so far, and those few are primarily polarity-switchable or fluorophilicity-switchable. Solvent switchability is desirable for processes in which consecutive operations (a reaction followed by a separation reaction followed by another reaction, or an extraction followed by a precipitation) require a change in solvent; the solvent that allows the first

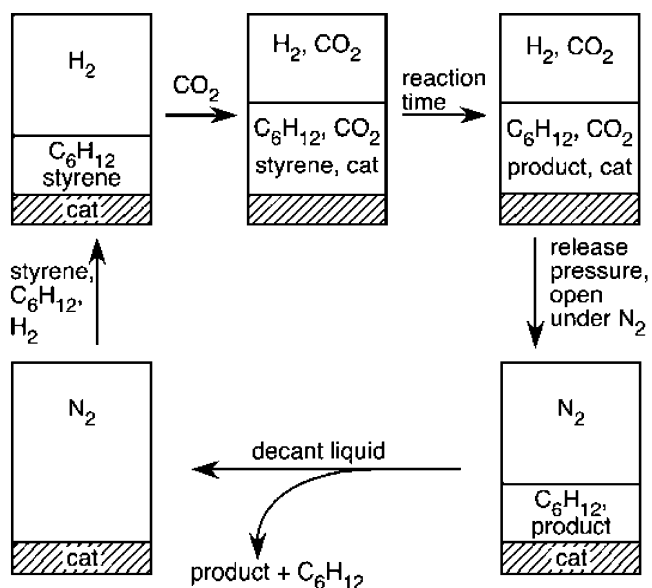


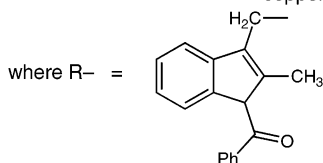
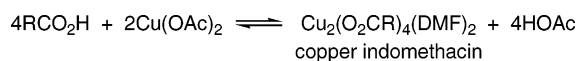
Figure 20. Hydrogenation and catalyst recycling using CO₂ as a solubility switch and fluoruous silica as a catalyst reservoir. The hatched area represents the fluoruous silica phase.²⁶¹

step to perform optimally is not the same as the solvent that allows the second step to perform optimally. For example, if a polar solvent is necessary for a particular extraction, but a much less polar solvent would make it much easier to subsequently separate the product from the solvent, then the ability to switch the solvent from polar to relatively nonpolar would be advantageous.

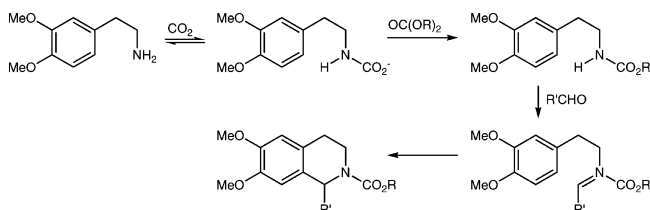
Polarity-switchable solvents fall into three groups: (a) supercritical fluids with significant dipole moments, (b) atmospheric pressure switchable solvents, and (c) gas-expanded solvents. The first two groups, which fall outside the scope of this review, can be summarized very briefly. Supercritical fluids that have significant dipole moments can be used as switchable solvents because their bulk polarity (as measured by the dielectric constant,^{262–265} for example) is a strong function of the temperature and pressure. Adjusting the dielectric constant by changing the pressure has a direct effect on reaction performance in these solvents.^{266,267} The first atmospheric pressure switchable solvent reported was a low-polarity liquid mixture of an amidine and 1-hexanol, which becomes polar under an atmosphere of CO₂ but switches back to low polarity in the absence of CO₂.^{18,268} Other switchable solvents are now known, including a primary amine/amidine mixture²⁶⁹ and secondary amines (without amidines).²⁷⁰ The third group, the expanded solvents, is the topic of this review, although expanded solvents are rarely described as switchable solvents. The fact that the polarity of expanded solvents can be readily changed was noted in section 2.4.1. Examples of the use of solvent expansion to trigger postreaction separations are described in section 3.5.

Fluorophilicity-switching of solvents have also been reported. CO₂ expansion of fluorophobic organic solvents causes them to become fluorophilic. This switch to fluorophilic is entirely reversible upon release of the CO₂ pressure. Such switching can be used to dissolve and then recrystallize fluorinated solids for the purposes of purification or crystallography.^{244,271} Fluorophilicity-switching of solvents has also been used in a scheme for homogeneous catalysis followed by a catalyst/product separation (section 3.5).

Scheme 2. The Equilibrium in the Preparation of Copper Indomethacin²⁷²



Scheme 3. The Pictet Spengler Reaction Performed in CO₂-Expanded Neat Substrate²⁷⁴



Solid/liquid switching of a solvent has been used to protect air-sensitive homogeneous catalysts from degradation.²² Wilkinson's catalyst ($\text{RhCl}(\text{PPh}_3)_3$) dissolved in CO_2 -expanded poly(ethylene glycol) (PEG) can be used to promote the hydrogenation of alkenes. The PEG solvent is liquid under the reaction conditions because of the melting-point lowering effect of the dissolved CO_2 . However, once the CO_2 pressure is released, the PEG freezes, encapsulating the catalyst and protecting it from reacting with air. Catalyst encapsulated inside PEG in this manner can be stored in open air, while the same catalyst as a pure powder or dissolved in a normal liquid solvent loses its activity when stored in air.

3.7. Uncatalyzed Reactions

3.7.1. Using Expansion To Shift Equilibria

Selective precipitation of a product by using CO_2 as an antisolvent can be used to drive an equilibrium reaction. This was the principle behind Foster's synthesis of copper indomethacin in CO_2 -expanded DMF (Scheme 2).²⁷² A phase behavior study showed that expanding DMF with CO_2 would cause copper indomethacin to precipitate at pressures below those necessary to precipitate the other species in the equilibrium.

The liquid-phase uncatalyzed esterification of acetic acid with ethanol (eq 2) was found to give a slightly greater conversion when the neat reaction mixture was expanded with CO_2 (60 °C, 59 bar). A possible explanation was the partial evaporation of the product ester into the CO_2 -rich vapor phase, which could drive the equilibrium further to the right.²⁷³



In order to promote an overall Pictet Spengler reaction, Dunetz et al. used the high concentration of CO_2 in expanded neat substrate to help drive the conversion of an amine to a carbamate salt (first step of Scheme 3). The carbamate was then converted by a carbonate ester and an aldehyde into an acyliminium that is particularly activated toward the Pictet Spengler reaction.²⁷⁴ The yield of tetrahydroisoquinoline increased with increasing CO_2 pressure up to 120–130 bar, but at 180 bar, a lower yield was obtained presumably

because the supercritical CO_2 removed much of the dialkylcarbonate from the liquid phase.

3.7.2. Using Expansion To Promote Polymerization

Free-radical polymerization of styrene in CO_2 -expanded THF gives lower molecular weights and slightly narrower molecular weight distributions than in unexpanded THF (even with correction for the dilution caused by expansion).²⁷⁵ The gel effect, in which polymer molecular weights are increased because the solution viscosity becomes quite high during the polymerization, was not observed in the expanded liquid, possibly because of the viscosity-lowering effect of the CO_2 . Similar tests of the polymerization of methyl methacrylate (MMA) in CO_2 -expanded solvents also gave lower M_w with increased pressure, but the polydispersity increased.^{276,277} At the highest expansions, bimodal distributions were observed. For both styrene and MMA polymerization, precipitation of polymer was observed at the higher CO_2 pressures.

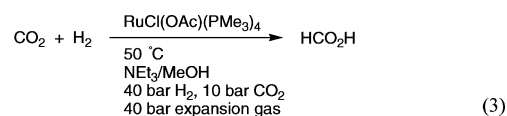
Ultrasound can be used as an initiator of free-radical polymerizations, but increasing viscosity of the liquid phase as the polymerization proceeds causes a drop in the rate of reaction. The ultrasound initiates radical formation due to the high temperatures and shear induced during cavitation, but cavitation is hindered by high viscosity.²⁷⁸ Even very low pressures of 1–7 bar of CO_2 are sufficient to prevent the slowing of the reaction and increase the conversion and the molecular weight of poly(methyl methacrylate) prepared in expanded monomer.^{279,280}

3.8. Homogeneous Catalysis

3.8.1. Hydrogenation

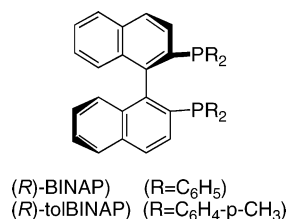
Hydrogenations can benefit from CO_2 -expansion of the solvent in many ways, as will be described. However, one benefit that has not been publicized but is universally appealing is an increase in safety. As has been shown in reaction studies, a CO_2/H_2 mix can be just as effective chemically as pure H_2 at the same total pressure. From a safety standpoint, the mixture is greatly preferred. Fires and explosions that occur because of accidental emissions of H_2 could be either prevented or at least ameliorated by the presence of CO_2 in the mixture.

Jessop's group³⁹ investigated the effect of the choice of expansion gas on the rate of hydrogenation of CO_2 in liquid MeOH/NET_3 mixture (eq 3). The turnover frequency was 770 h^{-1} with no expansion gas, but dropped to 160 h^{-1} when ethane (40 bar) was added, and rose to 910 h^{-1} when CHF_3 was used as the expansion gas. The low polarity of ethane was blamed for the decreased rate in the ethane-expanded solvent; an experiment with added liquid hexane produced a similar depression in the rate. Therefore, the properties of the expanding gas, rather than simply its presence, have an effect on reaction performance in the expanded solvent.



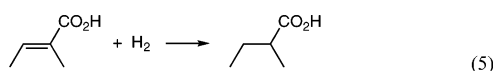
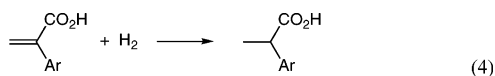
Expansion of solvents as a method for making H_2 more available to homogeneous catalyzed reactions is particularly of interest in asymmetric hydrogenations. The systems most studied in this context are the hydrogenations of α,β -unsaturated carboxylic acids catalyzed by Ru BINAP com-

Scheme 4. The Structures of BINAP and tolBINAP Ligands

Table 5. Asymmetric Hydrogenation of Atropic and Tiglic Acids at 25 °C in [bmim]PF₆ with and without Expansion by CO₂²⁸⁷

substrate	H ₂ , bar	CO ₂ , bar	e.e., %
Tiglic acid	5	0	93
	5	70	79
Atropic acid	50	0	32
	50	50	57
	100	0	49

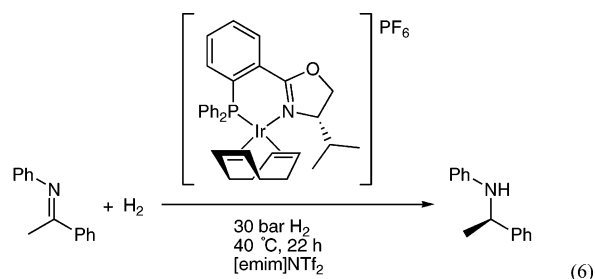
plexes such as Ru(OAc)₂(BINAP) (Scheme 4). The enantioselectivities of those hydrogenations are strongly dependent on the availability of H₂ in solution.^{281,282} For some substrates such as atropic acids (2-arylacrylic acids (eq 4), the more available the H₂, the higher the selectivity. For others, such as tiglic acid (2-methyl-2-butenoic acid, eq 5), more available H₂ results in lower selectivity. Foster's group²⁸³ investigated the asymmetric hydrogenation of 2-(6'-methoxy-2'-naphthyl)-acrylic acid, which is an atropic acid, in CO₂-expanded methanol with [RuCl₂(BINAP)(cymene)]₂, finding the reaction faster but less selective than in normal methanol.²⁸⁴ A subsequent study²⁸⁵ using RuCl₂(BINAP) catalyst reported that the reaction in expanded methanol was slower than in normal methanol.



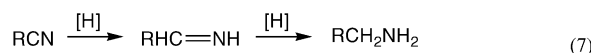
The influence of CO₂-expansion on hydrogenations in ILs is particularly interesting because the little data available so far suggests that ILs are very poor at dissolving H₂ gas.²⁸⁶ It therefore comes as no surprise that good enantioselectivities are obtained for tiglic acid²⁸⁷ and poor selectivity is obtained for atropic acids in pure ILs.^{287,288} CO₂-expanded ILs are much better¹³³ at dissolving H₂ and are also likely to have more rapid diffusion of the H₂ into the liquid phase. This combination of changes makes H₂ far more available to reactions in the IL and could therefore improve rates and change reaction selectivities. This was illustrated for asymmetric hydrogenations by work done in a collaboration between Jessop, Liotta, and Eckert.²⁸⁷ The hydrogenation of tiglic acid in [bmim]PF₆ is superior in enantioselectivity to that in CO₂-expanded [bmim]PF₆ (Table 5), because tiglic acid is hydrogenated in greater selectivity when H₂ is at low concentrations in solution. However, the hydrogenation of atropic acid is greatly improved in selectivity when the IL is expanded. In fact, a H₂/CO₂ mixture gave greater enantioselectivity than pure H₂ at the same total pressure.

The effect of CO₂-expansion on the rate of hydrogenations in ILs was measured by Leitner's group.¹³³ Hydrogenation of *N*-(1-phenylethylidene)aniline (eq 6) proceeded to only 3% conversion in 22 h in [emim]NTf₂ and to >99% in CO₂-

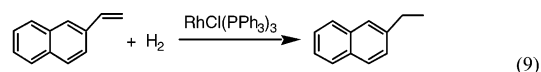
expanded [emim]NTf₂. The effect of CO₂ expansion was attributed to the much greater availability of H₂ to the catalyst in the liquid phase.



Homogeneous hydrogenation of nitriles to primary amines (eq 7) is facilitated in CO₂-expanded THF compared to normal THF because the CO₂ converts the amine product into the insoluble carbamate salt (eq 8). This salt can then be removed by filtration and reconverted to the amine by heating. Isolated yields are improved by this method.²⁸⁹

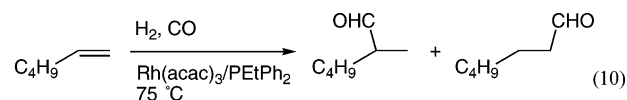


Solventless reactions of solids are typically slow because of poor mass transfer, but are environmentally preferable to reactions performed in liquid solvents. While it is possible to solve the mass transfer limitations by heating up the reaction to cause one reagent to melt, this approach is not desirable for thermally sensitive reagents or for reactions that have inferior selectivity at higher temperatures. An alternative is to lower the melting point of one of the reagents by adding CO₂ gas. This has been proven effective for the hydrogenation (eq 9) and hydroformylation of vinyl naphthalene at a temperature 33 °C below its melting point.²⁹⁰ Similarly, solventless reactions of liquid reagents can have mass transfer limitations if the product(s) are solids at the operating temperature. Again, CO₂ gas allows the reaction to proceed (see reaction 13 in section 3.9.1).²⁹⁰



3.8.2. Hydroformylation

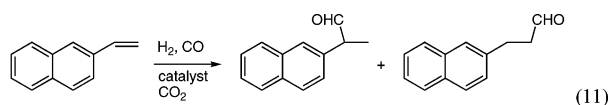
Abraham's group²⁹¹ found that the homogeneously catalyzed hydroformylation of 1-hexene (eq 10) in CO₂-expanded toluene was more rapid than in *sc*CO₂ but slower than in normal toluene. The high CO₂ pressure used was sufficient to dissolve some of the 1-hexene out of the liquid phase into the CO₂ phase, thereby lowering the concentration of hexene available to the catalyst.



Jin and Subramaniam¹⁸² demonstrated homogeneous hydroformylation of 1-octene using an unmodified rhodium catalyst (Rh(acac)(CO)₂) employing CXLs as reaction media. At 60 °C, the turnover numbers (TONs) for aldehydes formation in CO₂-expanded acetone were significantly higher than those obtained in either neat acetone or *sc*CO₂, demonstrating that CXLs are optimal reaction media. The regioselectivity toward linear and branched aldehydes (*n*/

iso ratio) remains unaffected by the change in either the solvent media or the temperature. The observed effects of temperature and H₂ concentration in CXL media are similar to those reported in the literature: lower temperatures favored the selectivity toward the aldehydes, while an increase in H₂ concentration resulted in a higher reaction rate. In follow-up studies,¹²⁸ the performance of several rhodium catalysts, Rh(acac)(CO)₂, Rh(acac)[P(OPh)₃]₂, Rh(acac)(CO)[P(OAr)₃] and two phosphorus ligands, PPh₃ and biphephos, was compared in neat organic solvents and in CXLs wherein more than 50% of the solvent volume is replaced with dense CO₂ at relatively mild temperatures (30–90 °C) and pressures (<120 bar). For all catalysts, enhanced turnover frequencies (TOFs) were observed in CXLs. For the most active catalyst, Rh(acac)(CO)₂ modified by biphephos ligand, the selectivity to aldehyde products was improved from approximately 70% in neat solvent to nearly 95% in CXL media. The enhanced rates and selectivity are attributed to increased syngas availability in the CXL phase. In experiments performed without added solvent, a TOF maximum was observed at an optimum CO₂ content. It appears that at higher than optimum CO₂ content, the TOF decreases due to dilution of substrate by CO₂, while at lower than optimum values the TOF is limited by reduced syngas availability in the CXL phase. The observed TOF (~300 h⁻¹), *n/i* ratio (>10), and aldehydes selectivity (~90%) at the optimum CO₂ content were either comparable to or better than values reported with other media and catalysts. Furthermore, the operating pressure (38 bar) and temperature (60 °C) for the CXL process are significantly milder than those reported for industrial hydroformylation processes.¹²⁸

Melting of a solid substrate by dissolution of CO₂ was shown by Jessop's group to be an effective way of performing a solventless hydroformylation of vinyl naphthalene (eq 11).²⁹⁰ An enantioselective version of the same reaction has also been performed in this manner.²⁹²

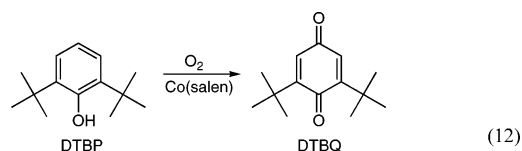


Recently the use of CO₂-IL biphasic media for continuous-flow hydroformylation has been reported.^{293–295} Typically, the active catalysts are immobilized in a stationary IL phase, and the syngas and the substrate are dissolved in a mobile *sc*CO₂ phase. The dense CO₂ phase transports the substrate and reactant gases into the IL while stripping the product from the IL. During the continuous runs performed by Cole-Hamilton's group, constant activity for up to 3 days was demonstrated in 1-octene hydroformylation catalyzed by a [pmim][Ph₂P(3-C₆H₄SO₃)] modified Rh catalyst in [bmim]PF₆/*sc*CO₂ biphasic media (where "pmim" is 1-*n*-propyl-3-methylimidazolium). Compared to the industrial cobalt-catalyzed processes, higher TOFs were observed; the selectivity to linear aldehyde (70%) is comparable to those attained in the industrial processes (70–80%). However, the authors point out that the air/moisture sensitivity of the ILs and the ligands may lead to the deactivation and leaching of the rhodium catalyst.

3.8.3. Oxidation Using O₂

The Subramaniam/Busch team has shown in several studies the rate and safety advantages of expanded liquids for oxidations. The homogeneous catalytic O₂-oxidation of

2,6-di-*tert*-butylphenol, DTBP, by Co(salen*) was studied in *sc*CO₂, in CO₂-expanded acetonitrile (*V/V*₀ = 2), and in the neat organic solvent (eq 12).^{44,296} The TOF in the CO₂-expanded MeCN (at 60–90 bar) is between 1 and 2 orders of magnitude greater than in *sc*CO₂ (at 207 bar). The observed selectivity toward DTBQ (80–88%) is comparable in *sc*CO₂ and CO₂-expanded MeCN, and no MeCN oxidation was detected in either case. The TOF and DTBQ selectivity are lower in neat MeCN (O₂ bubbling, 28 °C, 1 bar). Neat solvents can form explosive gaseous mixtures at higher temperatures and hence were studied only at ambient temperature. The less expensive and readily available Co(salen) catalyst is insoluble in *sc*CO₂ but shows remarkable activity in CO₂-expanded MeCN. These results clearly show that CO₂-expanded solvents advantageously complement *sc*CO₂ as reaction media by broadening the range of conventional catalyst/solvent combinations with which homogeneous oxidations by O₂ can be performed.

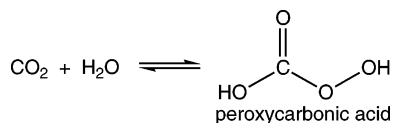


Taking advantage of the better solvent power of CXL (compared to *sc*CO₂), the oxidation of cyclohexene by O₂ was investigated with a nonfluorinated iron porphyrin catalyst, (5,10,15,20-tetraphenyl-21*H*,23*H*-porphyrinato)iron(III) chloride, Fe(TPP)Cl, in addition to a fluorinated catalyst (5,10,15,20-tetrakis(pentafluorophenyl)-21*H*,23*H*-porphyrinato)iron(III) chloride, Fe(PFTPP)Cl.⁴⁴ While Fe(TPP)Cl is insoluble and displays little activity in *sc*CO₂, it displays high activity in CO₂-expanded MeCN. The conversion histories of cyclohexene oxidation with Fe(TPP)Cl at 50 °C in CO₂-expanded MeCN (*V/V*₀ = 2) and in neat MeCN are each associated with an "induction" period, which presumably involves the buildup of radicals to a critical concentration. Remarkably, the induction period in CO₂-expanded MeCN is only 4 h compared to nearly 16 h in neat MeCN. This reduced induction period was attributed to the enhanced O₂ solubility in CO₂-expanded MeCN, assuming that the free radical initiation step involves molecular oxygen. Further, the cyclohexene conversion obtained with the fluorinated catalyst Fe(PFTPP)Cl in the CO₂-expanded solvent at 90 bar and 80 °C is 41% which is nearly 7-fold greater than that reported⁸ for *sc*CO₂ with the identical catalyst at the same temperature (at 345 bar). Also, an approximately 1.5-fold higher epoxidation selectivity over *sc*CO₂ is obtained in CO₂-expanded CH₃CN.

Cyclohexene conversion and product selectivity also depend on the CO₂-fraction in the reaction medium. Conversion increases from 24% in neat CH₃CN to a maximum of 31%, at 2-fold expansion, decreasing upon further CO₂-expansion. Epoxidation selectivity showed a similar trend. While the changes are not dramatic, they do indicate that a continuum of reaction media with different properties is realized by varying the CO₂/solvent ratio, and that the ratio may be optimized for a given process through a combination of solubility effects and solvent properties.

3.8.4. Oxidation Using H₂O₂

Richardson's group showed that epoxidation of alkene can be achieved using the percarbonate ion which is formed by reaction of H₂O₂ and sodium carbonate under basic condi-

Scheme 5. *In Situ* Formation of Oxidant for the Epoxidation of Olefins in CXLs

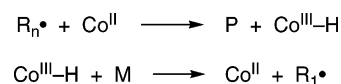
tions.²⁹⁷ The Eckert/Liotta group showed that the reaction between H_2O_2 and CO_2 yields a peroxycarbonic acid species (Scheme 5), an oxidant that facilitates olefin epoxidation.^{298,299} Beckman's group^{297,300,301} reported relatively low conversion ($\sim 3\%$) of propylene to propylene oxide (PO) using percarbonate formed in a biphasic system via reaction of CO_2 and H_2O_2 with NaOH as a base. The low conversions are typical of mass transfer limitations in biphasic systems.

The Subramaniam/Busch team showed that the miscible regions (in P-T-x space) for water/solvent/ CO_2 ternary systems can be elegantly exploited for performing homogeneous catalytic oxidation of organic substrates by water-soluble catalysts and oxidants.²³ By the employment of CO_2 -expanded $\text{CH}_3\text{CN}/\text{H}_2\text{O}_2/\text{H}_2\text{O}$ homogeneous mixtures, it was shown that a variety of olefin epoxidation reactions may be performed in a homogeneous CO_2 -expanded phase containing the olefin, CO_2 , and H_2O_2 (in aqueous solution), thereby alleviating the interphase mass transfer limitations associated with biphasic systems. By the employment of pyridine as the base to stabilize the peroxy acids, 1 to 2 orders of magnitude enhancement in epoxidation rates (compared to the biphasic system) was achieved with $>85\%$ epoxidation selectivity.²³

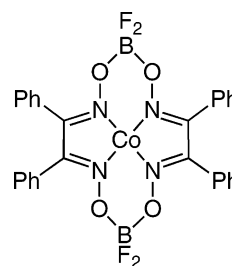
Recently, the Busch and Subramaniam groups investigated propylene oxidation by creating a homogeneous mixture of dense CO_2 , an organic solvent such as acetonitrile or methanol, and water.³⁰² Such a mixture should also enhance the solubility of propylene, and therefore its availability, in the liquid phase. When pyridine is used as a base, the PO yield at $40\text{ }^\circ\text{C}$ is on the order of 10% after 12 h at roughly 48 bar. In the presence of an added catalyst (methyltrioxorhenium or MTO), the PO yield is significantly enhanced to 80% in 3 h with PyNO as the base. It was found that when $\text{N}_2/\text{C}_3\text{H}_6$ (instead of $\text{CO}_2/\text{C}_3\text{H}_6$) was used as the pressuring medium over the homogeneous $\text{H}_2\text{O}_2/\text{H}_2\text{O}/\text{MeOH}/\text{PyNO}$ mixture containing dissolved catalyst, remarkably high activity (92% PO yield in 1 h) was achieved at approximately 14 bar. Because lower olefins exhibit high solubility in aqueous media, it seems plausible that the CO_2 swelling of the reaction phase lowers the reactant concentration. Thus, N_2 is the preferred gas in this case. Furthermore, the PO may be easily separated from the aqueous phase by distillation, thereby recycling the catalyst.

3.8.5. Polymerization

Catalytic chain transfer polymerizations are free-radical polymerizations with a mechanism for keeping the chain lengths short; a homogeneous catalyst is used to terminate one chain and start a new one. Chain transfer, catalyzed by cobalt complex **2** during the polymerization of methyl methacrylate, is suspected of being a diffusion-controlled reaction in which the Co(II) catalyst abstracts a hydrogen atom from the polymer radical ($\text{R}\bullet$) and later transfers it to a monomer to start the growth of a new polymeric chain (Scheme 6). Zwolak et al.³⁰³ reported that the rate of chain transfer during this polymerization was 4-times greater in CO_2 -expanded methyl methacrylate (60 bar, $50\text{ }^\circ\text{C}$) than in

Scheme 6. The Catalytic Chain Transfer Mechanism³⁰³

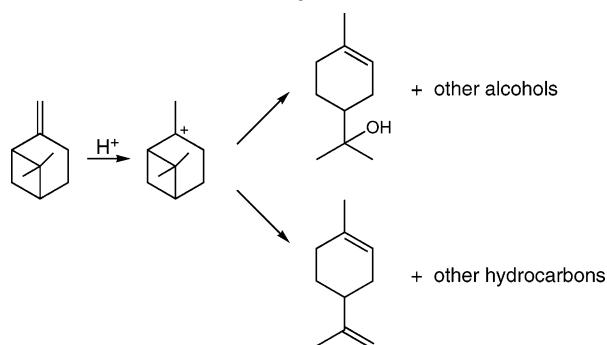
neat monomer. The improved rate was attributed to the lowered viscosity of the expanded solution.

**3.9. Heterogeneous Catalysis**

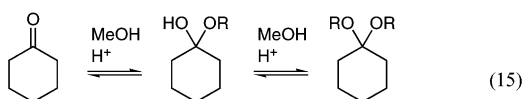
Many of the attributes of GXLs exploited in homogeneous reaction systems are also applicable in heterogeneous catalysis. For example, adding CO_2 to an organic liquid phase (in many cases a significant fraction of the reaction medium is replaced with compressed CO_2) in a fluid–solid catalytic system should enhance gas solubilities and improve mass transfer properties of the newly created CXL phase. Similarly, two immiscible liquid phases may be reduced to a single phase by adding a third liquid solvent in which the two phases exhibit mutual solubility. Following reaction, immiscibility of the two phases may be triggered by either temperature and/or addition of a mass separation agent (such as compressed CO_2). Reviews of near-critical and supercritical phase heterogeneous catalysis may be found elsewhere.^{304–307}

3.9.1. Hydrogenations

As shown by the Roberts' group, the conditions required to form a single supercritical phase may not be suitable for some hydrogenation processes.³⁰⁸ In such cases, CXL media may be an alternative, since they exhibit better mass transport properties (lower viscosity and higher diffusion coefficients) than unexpanded liquids. Furthermore, higher H_2 solubility in a CO_2 -expanded liquid has been reported at certain conditions (section 2.5.2). Employing dense CO_2 as the solvent medium, Devetta et al.³⁰⁹ systematically investigated the $\text{Pd}/\text{Al}_2\text{O}_3$ hydrogenation of unsaturated ketones in a stirred reactor and reported that the hydrogenation rate of the CO_2 -expanded ketone was higher than that of the unswollen ketone. Chouchi and co-workers³¹⁰ reported that during the Pd/C hydrogenation of pinene in $s\text{cCO}_2$, the reaction rate was higher at much lower pressures (where a condensed phase exists) compared to single-phase operation at supercritical conditions. This result is similar to the significantly enhanced oxidation rates at intermediate pressures (where two phases exist) reported by Baiker's group during a study of $\text{Pd}/\text{Al}_2\text{O}_3$ -catalyzed partial oxidation of octanol.³¹¹ It would appear that, in these examples, the reactions in condensed phases benefit from the earlier described advantages of performing reactions in CO_2 -expanded phases. More recently, the rate constant for the hydrogenation of the aromatic rings in polystyrene (PS) was found to be higher in CO_2 -expanded decahydronaphthalene (DHN) than in neat DHN.³⁰⁸ Recently, Chan and Tan³¹² reported enhanced rates in the presence of compressed CO_2

Scheme 8. The Hydrolysis of β -Pinene

higher pressures are inferior due to the decreasing polarity of the expanded solvent inhibiting the dissociation of the acid.



In situ acids are also capable of catalyzing the hydrolysis of β -pinene to terpineol and other alcohols with good selectivity for alcohols rather than hydrocarbons (Scheme 8).³²⁰ The reaction was performed in CO_2 -expanded 1:1 MeOH/ H_2O mixture (75 °C, 3 mol % CO_2). The reaction fails if the CO_2 is omitted.

Addition of CO_2 to high-temperature water accelerates reactions that can proceed by acid catalysis. Poliakoff's group³²¹ found that CO_2 dissolved in water at 250 °C promotes the decarboxylation of benzoic acid. Hunter and Savage^{121,322} have used dissolved CO_2 to acid-catalyze the dehydration of cyclohexanol to cyclohexene and the alkylation of *p*-cresol to 2-*tert*-butyl-4-methylphenol. In both cases, the yield (after a short reaction time) was double that in the absence of CO_2 . Hydration of cyclohexene to cyclohexanol at 300 °C showed a 5-fold increase in initial rate as the pressure of CO_2 was increased from 0 to 55 bar.³²²

3.11. Other Applications

The creativity of researchers in the field continues to lead to new applications of gas-expanded liquids. The following applications may indicate future areas of research and industrialization.

Sarrade et al.¹¹⁴ showed that the dramatic viscosity reduction in oils upon expansion with CO_2 could be applied to the ultrafiltration of used motor oils through a membrane, giving an energy-efficient method for oil re-purification.

Atomization of fuels in combustion engines can be improved by dissolution of CO_2 in the fuel, because of the reduction in viscosity.³²³ Refrigeration Freon gases have been found to lower the viscosity of lubricating oils inside refrigeration compressors.³²⁴

Expanded liquids can be used as solvents for removing photoresists during the manufacture of integrated circuits.³²⁵ The expanded liquids are preferable to traditional liquids because of the lower viscosity, which is particularly important for circuits containing nanoscale structures.

4. Process Engineering Issues

In a 2000 review, Perrut³²⁶ provided an overview of the industrial applications of supercritical CO_2 and economic issues thereof. Beckman³⁰⁷ provided a broad perspective of

the process design issues and challenges facing commercialization of CO_2 -based plants. There are many industrial-scale, CO_2 -based plants worldwide in the food and natural products industries (such as the decaffeination of coffee beans, extraction of hops and spices, etc.). Other industrial applications include dry cleaning and precision cleaning,^{327–329} paints and coatings (Union Carbide process), polymer processing (DuPont Fluoropolymers Plant), and hydrogenations.³³⁰ In contrast, there are relatively few known examples of commercialization in the areas of chemical manufacturing and particle formation processes employing dense CO_2 , despite nearly two decades of research in these areas and the promise of many potential applications. This lack of commercialization cannot be solely linked to the need for employing high pressures in CO_2 -based processes considering that current industrial applications involving dense CO_2 employ such high pressures and many industrial processes such as hydroformylation of higher olefins (~ 200 bar). One may therefore conclude that a main impediment to commercialization is the lack of clarity in projecting process economics and/or demonstrating satisfactory pilot plant scale performance, both of which are essential for industries to make business decisions for continued development and deployment of technologies on a commercial scale.

As with any process development, fundamental knowledge of essential process parameters is essential to perform reliable simulations and economic analysis of GXL processes. Specifically, reliable knowledge of solution phase behavior, physical and thermodynamic properties, intrinsic kinetics and mechanistic parameters, fluid dynamics, and transport properties (diffusivity, viscosity, interfacial tension) involving GXLs is essential for process design and optimization. In many GXL application areas, the fundamental data and/or experimental and theoretical tools required for acquiring such data are either not readily available or nonexistent. This is especially true for chemical conversion and particle formation processes involving dense CO_2 , where commercialization activity has been relatively sparse and slow. The range of expertise required for thoroughly addressing these issues encompasses both the chemical science and engineering disciplines. During the past decade, the field has witnessed an increasing number of such interdisciplinary collaborations at research centers such as those at the Georgia Institute of Technology, University of Nottingham, RWTH (University of Aachen), University of North Carolina, University of Pittsburgh, and the University of Kansas, to mention a few. As reviewed in the previous sections, these and several other groups are making significant advances in addressing fundamental and process engineering issues, and developing broad enabling tools that are aiding quantitative economic and environmental assessment of GXL processes.

In homogeneous catalysis applications, many groups report that the preferred operating pressures for GXL processes (wherein both reaction and environmental benefits are optimized) are on the order of tens of bars (see section 3.8). Also, the concentrations of organic substrates and catalysts are typically higher in a GXL phase relative to a supercritical phase. Further, permanent gas solubilities in GXL phases are either enhanced or retained when the reactant gas (CO , H_2 , or O_2) is partially replaced by CO_2 such that the total pressure is constant. In many examples, such "tuning" of the concentrations of reactants in GXL phases has been exploited to maximize the turnover frequency at mild pressures. As discussed in section 3.8.2, in the case of the

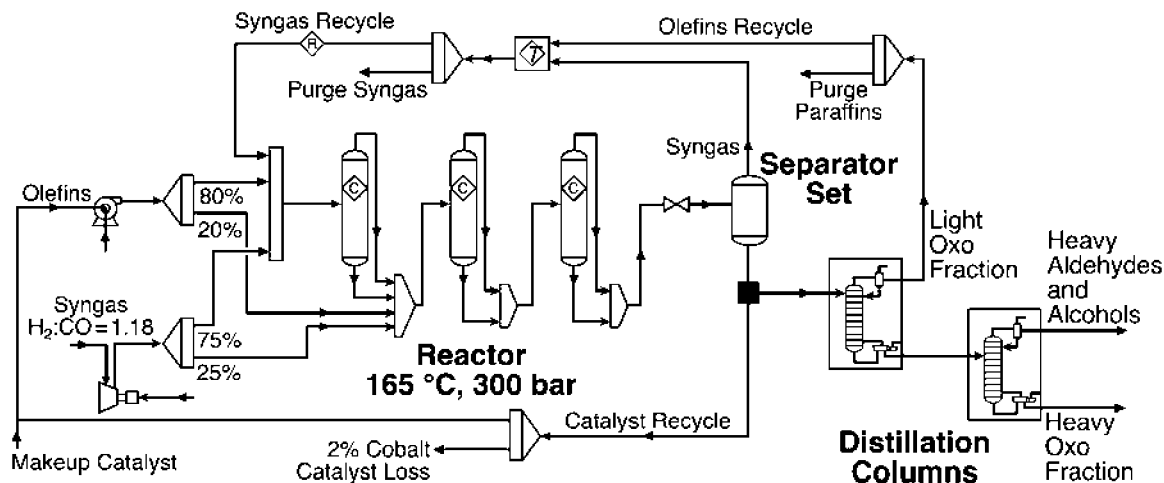


Figure 21. Process flow diagram for the Exxon hydroformylation process.

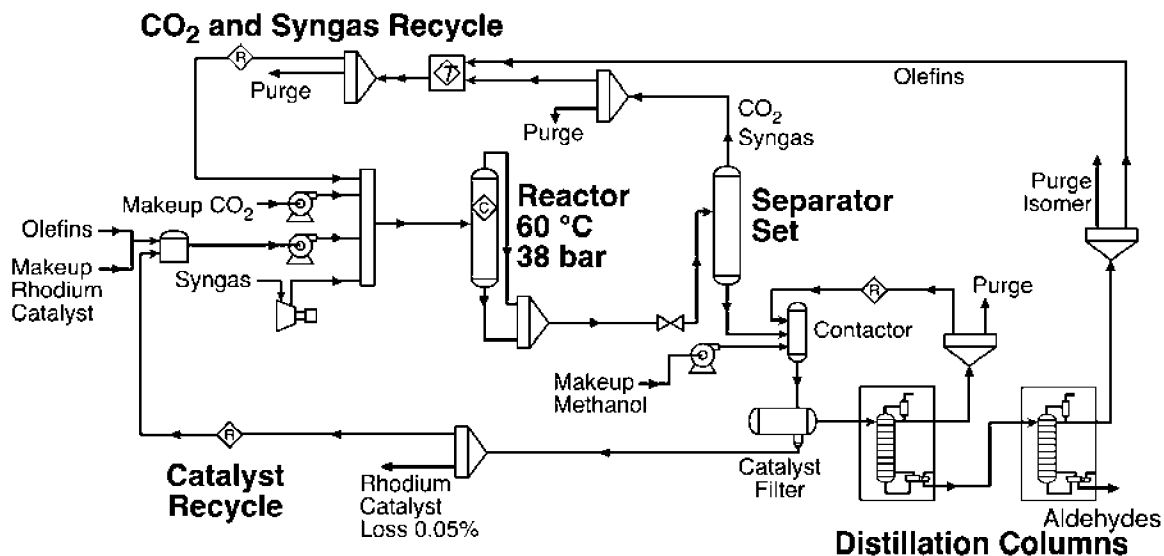


Figure 22. Process flow diagram for the CXL-based hydroformylation process.

hydroformylation of higher olefins, the required optimum pressures in GXL-based processes are significantly lower (~ 40 bar) than those required for conventional processes (~ 200 bar).¹²⁸ Process intensification at lower pressures generally tends to favor process economics and is generally considered to be inherently safer and environmentally friendlier. However, these conclusions must be supported by quantitative comparisons of the relative economics of the GXL and competing processes; the separation/recycle of catalysts from the GXL streams, product recovery, and the subsequent recycle of CO_2 may adversely affect economics. Quantitative analyses, even at the early research stage of process development, can provide valuable process engineering and research guidance by establishing performance targets (operating pressure range, temperature range, extent of catalyst recovery, product purity, etc.) that must be met to ensure economic viability of new processes. An example of such an analysis of a CXL-based hydroformylation process is provided by Fang et al.³³¹

On the basis of assumptions detailed in the referenced article,³³¹ the Exxon and CXL processes were simulated with Aspen HYSYS 2004.2 software for quantitative evaluation of the processes. The common design basis is a production rate of 45 000 tons/year of desired product aldehydes and alcohols,³³² and the composition of olefin feedstock is taken

from the Exxon patent US 4 658 068.³³³ For the Exxon process (Figure 21), the pressurized olefins and syngas mixture (at 300 bar) are fed through the loop reactors.³³⁴ The unreacted syngas and olefins are separated, recompressed, and recycled as shown schematically in Figure 21. Product is distilled in three stages: Light Oxo Fraction (LOF), Heavier Aldehydes and Alcohols (HA), and Heavy Oxo Fraction (HOF). Because of a lack of adequate plant data, the catalyst recycle, hydrogenation, and steam-cracking steps are not considered in this preliminary simulation. Figure 22 is the schematic of a CXL process. The CO_2 , unreacted syngas, and olefins are separated, recompressed, and recycled. The catalyst complex (polymer-bound, bulky-phosphite-modified rhodium catalyst) is precipitated by adding methanol into relatively nonpolar crude product and then filtered.

Cost estimations reveal that the total production costs of the CXL and the Exxon processes are comparable even though the CXL process uses a Rh-based catalyst. The CXL process has an approximately 25% lower total capital investment because of milder operating conditions (T and P) than the Exxon process, but this is offset largely by the higher Rh catalyst costs in the CXL process. The main economic driver in the CXL process is therefore the extent of recovery of the Rh-based catalyst. This conclusion is to

be intuitively expected given the fact that the Rh-based catalysts are nearly 1000-fold more expensive than the Co-based catalysts used in the Exxon process. Near-quantitative catalyst recovery is required for the CXL process economics to compete favorably with the Exxon Process. Such a catalyst recycle target is not unreasonable considering that near-total recovery (99.95%) of polymer-bound, bulky-phosphite-modified rhodium catalysts has been reported in the literature.³³⁵ The development of active and easily recyclable forms of the less expensive Co-based catalysts provides an even better opportunity to make the CXL-based process more competitive.

The higher selectivity in the CXL process decreases the *E*-factor or the environmental burden index. On the basis of the process flow diagrams (Figures 21 and 22), comparative environmental impact assessment may also be performed using tools such as the U.S. EPA's Environmental Fate and Risk Assessment Tool (EFRAT).³³⁶

5. Summary

Although gas-expanded liquids have been known in some form or other for some time, the realization in the research community of their potential in a wide range of applications has only happened in the past few years. Of the references cited in this review, 60% date from 2000 onward. This is despite the fact that the use of CO₂ as a viscosity-reducing agent for crude oil has been investigated since 1951 (see references within ref 219). Nevertheless, the creativity of the research community is now fully engaged, and there are already many examples of facilitated separations, reactions, materials processing, and particle formation. In virtually every application, the GXLs represent an enabling tool for effecting significant improvements in one or more process performance measures such as reaction rate, transport rate, product selectivity, product quality, and environmental friendliness. New research directions include cleaning, *in situ* acid-promoted reactions, and multifunctional CO₂-aided continuous catalytic reaction systems that integrate reaction and separation. Successful development of new technologies will require multi-scale interdisciplinary research collaborations involving scientists and engineers.

There are gray areas between expanded liquids and supercritical fluid mixtures that have not been discussed in this paper. For example, the CO₂/coating material mixtures that are used in CO₂-based spray coating systems are usually described as being supercritical, but they may not be supercritical in comparison to the true critical point of the mixture. CO₂/liquid mixtures of all kinds, whether expanded, supercritical, or both, will continue to be applied in new areas, including many that have not yet been imagined.

Industrialization of expanded liquids has started in applications requiring viscosity reduction (e.g., crude oil recovery). Future commercial applications that exploit viscosity reduction will be most likely in polymer processing and particle formation.

We plan occasional updates of this review in accord with the new "living review" format supported by this journal. Preprints/reprints of relevant work and/or private communications are most welcome and will be incorporated with fitting acknowledgment.

6. Abbreviations

α Kamlett-Taft hydrogen-bond donating ability parameter
 β Kamlett-Taft hydrogen-bond accepting ability parameter

γ shear rate
 η shear viscosity
 π^* Kamlett-Taft polarity/polarizability parameter
 acac acetylacetonate
 AOT sodium bis-2-ethylhexylsulfosuccinate
 ASES Aerosol Solvent Extraction System
 BINAP 2,2'-bis(diphenylphosphino)-1,1'-binaphthyl
 toBINAP 2,2'-bis(di(*p*-tolyl)phosphino)-1,1'-binaphthyl
 bmim *N*-butyl-*N'*-methylimidazolium
 cat catalyst
 CXL CO₂-expanded liquid
 DELOS Depressurization of an Expanded Liquid Organic Solution
 DHN decahydronaphthalene
 DME dimethyl ether
 DMF dimethylformamide
 DTBP 2,6-di-*tert*-butylphenol
 DTBQ 2,6-di-*tert*-butylquinone
 EF enhancement factor
 EOR enhanced oil recovery
 EoS Equation of State
 GAS gas antisolvent
 GEMC Gibbs Ensemble Monte Carlo
 GXL gas-expanded liquid
 HA Heavier Aldehydes and Alcohols
 HOF Heavy Oxo Fraction
 IL ionic liquid
 LCSP lower critical solution pressure
 LLV liquid-liquid-vapor
 LOF Light Oxo Fraction
 MD molecular dynamics
 MHEL maximum homogeneous expansion level
 MLSR magnetically levitated sphere rheometer
 MMA methyl methacrylate
p-MOAP *para*-methoxyacetophenone
 MTO methyltrioxorhenium
 NRTL nonrandom, two-liquid (activity coefficient model)
 OATS organic-aqueous tunable solvents
 P pressure (generally gauge pressure)
 PBS poly(butylene succinate)
 PCA Precipitation with Compressed Antisolvent
 PDMS poly(dimethylsiloxane)
 PE polyethylene
 PEG poly(ethylene glycol)
 PFTPP 5,10,15,20-tetrakis(pentafluorophenyl)-21*H*,23*H*-porphyrinato
 PGSS Particles from Gas-Saturated Solution
 PLUSS Polymer Liquefaction Using Supercritical Solvation
 PMMA poly(methyl methacrylate)
 PO propylene oxide
 PP polypropylene
 PPG poly(propylene glycol)
 PR-EoS Peng-Robinson Equation of State
 PS polystyrene
 PVDF poly(vinylidene fluoride)
 PyNO pyridine *N*-oxide
 salen* *N,N'*-bis(3,5-di-*tert*-butylsalicylidene)1,2-cyclohexane-diiminato(2-)
*sc*CO₂ supercritical CO₂
 SCF supercritical fluid
 SEDS Solution-Enhanced Dispersion by Supercritical fluids
 S-L-G solid-liquid-gas
*T*_c critical temperature
 Tf trifluoromethylsulfonyl
*T*_g glass transition temperature
*T*_m melting temperature
 TOF turnover frequency (mol product per mol catalyst per h)
 TON turnover number (mol product per mol catalyst)
 TPP 5,10,15,20-tetraphenyl-21*H*,23*H*-porphyrinato

TTBDQ	3,5,3',5'-tetra- <i>tert</i> -butyl-4,4'-diphenquinone
UCSP	upper critical solution pressure
VLE	vapor-liquid equilibria
VOC	volatile organic compound
X	liquid-phase composition
Y	vapor-phase composition
w ₀	water/surfactant mole ratio

7. Acknowledgment

B.S. acknowledges NSF funding (EEC-0310689) and donors of the Dan F. Servey endowed chair for some of his group's research results presented in this paper. P.G.J. acknowledges funding from the Natural Sciences and Engineering Research Council of Canada and the support of the Canada Research Chairs program.

8. References

- Sheldon, R. A. *CHEMTECH* **1994**, *24*, 38.
- "Latest Findings on National Air Quality: 2002 Status and Trends," EPA Office of Air Quality Planning and Standards, Emissions, Monitoring, and Analysis Division, 2003.
- Tundo, P.; Anastas, P.; Black, D. S.; Breen, J.; Collins, T.; Memoli, S.; Miyamoto, J.; Poliakoff, M.; Tumas, W. *Pure Appl. Chem.* **2000**, *72*, 1207.
- DeSimone, J. M. *Science* **2002**, *297*, 799.
- Adams, D. J.; Dyson, P. J.; Tavener, S. J. *Chemistry in Alternative Reaction Media*; Wiley: Chichester, England, 2004.
- Eckert, C. A.; Liotta, C. L.; Bush, D.; Brown, J. S.; Hallett, J. P. *J. Phys. Chem. B* **2004**, *108*, 18108.
- Morgenstern, D. A.; LeLacheur, R. M.; Morita, D. K.; Borkowsky, S. L.; Feng, S.; Brown, G. H.; Luan, L.; Gross, M. F.; Burk, M. J.; Tumas, W. In *Green Chemistry: Designing Chemistry for the Environment*; Anastas, P. T., Williamson, T. C., Eds.; American Chemical Society: Washington, DC, 1996; Vol. 626.
- Chemical Synthesis Using Supercritical Fluids*; Jessop, P. G.; Leitner, W., Eds.; VCH/Wiley: Weinheim, Germany, 1999.
- Amandi, R.; Hyde, J.; Poliakoff, M. In *Carbon Dioxide Recovery and Utilization*; Aresta, M., Ed.; Kluwer: Dordrecht, Netherlands, 2003.
- Green Chemistry Using Liquid and Supercritical Carbon Dioxide*; DeSimone, J. M.; Tumas, W., Eds.; Oxford University Press: New York, 2003.
- Gordon, C. M.; Leitner, W. *Chim. Oggi* **2004**, *22*, 39.
- Beckman, E. J. *Environ. Sci. Technol.* **2002**, *36*, 347A.
- Licence, P.; Poliakoff, M. In *Multiphase Homogeneous Catalysis*; Cornils, B., Herrmann, W. A., Horváth, I. T., Leitner, W., Mecking, S., Olivier-Bourbigou, H., Vogt, D., Eds.; Wiley-VCH: Weinheim, Germany, 2005.
- Li, C.-J.; Chan, T.-H. *Organic Reactions in Aqueous Media*; Wiley: New York, 1997.
- Aqueous-Phase Organometallic Catalysis*; Cornils, B.; Herrmann, W. A., Eds.; Wiley-VCH: Weinheim, Germany, 1998.
- Wasserscheid, P.; Welton, T. *Ionic Liquids in Synthesis*; VCH-Wiley: Weinheim, Germany, 2002.
- Green Industrial Applications of Ionic Liquids*; Rogers, R. D.; Seddon, K. R.; Volkov, S., Eds.; Springer, Boston, MA, 2003.
- Jessop, P. G.; Heldebrant, D. J.; Xiaowang, L.; Eckert, C. A.; Liotta, C. L. *Nature* **2005**, *436*, 1102.
- Zhuang, H.-Z.; Zou, X.-W.; Jin, Z.-Z.; Tian, D.-C. *Physica B* **1998**, *245*, 110.
- Cui, Y.; Olesik, S. V. *Anal. Chem.* **1991**, *63*, 1912.
- Phillips, S.; Olesik, S. V. *Anal. Chem.* **2002**, *74*, 799.
- Heldebrant, D. J.; Witt, H.; Walsh, S.; Ellis, T.; Rauscher, J.; Jessop, P. G. *Green Chem.* **2006**, *8*, 807.
- Rajagopalan, B.; Wei, M.; Musie, G. T.; Subramaniam, B.; Busch, D. H. *Ind. Eng. Chem. Res.* **2003**, *42*, 6505.
- Kordikowski, A.; Schenk, A. P.; Van Nielsen, R. M.; Peters, C. J. *J. Supercrit. Fluids* **1995**, *8*, 205.
- In a binary mixture of 1 wt % CO₂ in poly(dimethylsiloxane) (MW = 10 000), the mole fraction of CO₂ is 70%!
- Panagiotopoulos, A. Z.; Reid, R. C. In *Supercritical Fluids—Chemical Engineering Principles and Applications*; Squires, T. G., Paulaitis, M. E., Ed.; American Chemical Society Symposium Series: Washington, DC, 1987; Vol. 329.
- Day, C.-Y.; Chang, C. J.; Chen, C.-Y. *J. Chem. Eng. Data* **1996**, *41*, 839.
- Bamberger, A.; Sieder, G.; Maurer, G. *J. Supercrit. Fluids* **2000**, *17*, 97.
- Byun, H. S.; Kim, K.; McHugh, M. A. *Ind. Eng. Chem. Res.* **2000**, *39*, 4580.
- Chen, J.; Wu, W.; Han, B.; Gao, L.; Mu, T.; Liu, Z.; Jiang, T.; Du, J. *J. Chem. Eng. Data* **2003**, *48*, 1544.
- Wu, J.; Pan, Q.; Rempel, G. L. *J. Chem. Eng. Data* **2004**, *49*, 976.
- Francis, A. W. *J. Phys. Chem.* **1954**, *58*, 1099.
- Fornari, R. E.; Alessi, P.; Kikic, I. *Fluid Phase Equilib.* **1990**, *57*, 1.
- Bartle, K. D.; Clifford, A. A.; Jafar, S. A.; Shilstone, G. F. *J. Phys. Chem. Ref. Data* **1991**, *20*, 713.
- Dohrn, R.; Brunner, G. *Fluid Phase Equilib.* **1995**, *106*, 213.
- Christov, M.; Dohrn, R. *Fluid Phase Equilib.* **2002**, *202*, 153.
- Houndonougbo, Y.; Jin, H.; Rajagopalan, B.; Wong, K.; Kuczera, K.; Subramaniam, B.; Laird, B. B. *J. Phys. Chem. B* **2006**, *110*, 13195.
- Jin, H. Ph.D. Dissertation, University of Kansas, 2006.
- Thomas, C. A.; Bonilla, R. J.; Huang, Y.; Jessop, P. G. *Can. J. Chem.* **2001**, *79*, 719.
- Diamond, L. W.; Akinfiev, N. N. *Fluid Phase Equilib.* **2003**, *208*, 265.
- Aki, S. N. V. K.; Mellein, B. R.; Saurer, E. M.; Brennecke, J. F. *J. Phys. Chem. B* **2004**, *108*, 20355.
- Guadagno, T.; Kazarian, S. G. *J. Phys. Chem. B* **2004**, *108*, 13995.
- Radosz, M. *Ber. Bunsen-Ges.* **1984**, *88*, 859.
- Wei, M.; Musie, G. T.; Busch, D. H.; Subramaniam, B. *J. Am. Chem. Soc.* **2002**, *124*, 2513.
- Mueller, S. G.; Al-Dahhan, M. H.; Dudukovic, M., *Ind. Eng. Chem. Res.* **2007**, in press.
- Xue, J.; Al-Dahhan, M.; Dudukovic, M. P.; Mudde, R. F. *Can. J. Chem. Eng.* **2003**, *81*, 375.
- Shukla, C. L.; Hallett, J. P.; Popov, A. V.; Hernandez, R.; Liotta, C. L.; Eckert, C. A. *J. Phys. Chem. B* **2006**, *110*, 24101.
- Houndonougbo, Y.; Guo, J.; Lushington, G. H.; Laird, B. *Mol. Phys.* **2006**, *104*, 2955.
- Li, H.; Maroncelli, M. *J. Phys. Chem.* **2006**, *110*, 21189.
- Kazarian, S. G.; Briscoe, B. J.; Welton, T. *Chem. Commun.* **2000**, 2047.
- Cadena, C.; Anthony, J. L.; Shah, J. K.; Morrow, T. I.; Brennecke, J. F.; Maginn, E. J. *J. Am. Chem. Soc.* **2004**, *126*, 5300.
- Anthony, J. L.; Anderson, J. L.; Maginn, E. J.; Brennecke, J. F. *J. Phys. Chem. B* **2005**, *109*, 6366.
- Urukova, I.; Vorholz, J.; Maurer, G. *J. Phys. Chem. B* **2005**, *109*, 12154.
- Huang, X.; Margulis, C. J.; Li, Y.; Berne, B. J. *J. Am. Chem. Soc.* **2005**, *127*, 17842.
- Blanchard, L. A.; Hancu, D.; Beckman, E. J.; Brennecke, J. F. *Nature* **1999**, *399*, 28.
- Kamlet, M. J.; Abboud, J. L.; Taft, R. W. *J. Am. Chem. Soc.* **1977**, *99*, 6027.
- O'Neill, M. L.; Kruus, P.; Burk, R. C. *Can. J. Chem.* **1993**, *71*, 1834.
- Lu, J.; Liotta, C. L.; Eckert, C. A. *J. Phys. Chem. A* **2003**, *107*, 3995.
- Fredlake, C. P.; Muldoon, M. J.; Aki, S. N. V. K.; Welton, T.; Brennecke, J. F. *Phys. Chem. Chem. Phys.* **2004**, *6*, 3280.
- Deye, J. F.; Berger, T. A.; Anderson, A. G. *Anal. Chem.* **1990**, *62*, 615.
- Baker, S. N.; Baker, G. A.; Kane, M. A.; Bright, F. V. *J. Phys. Chem. B* **2001**, *105*, 9663.
- Schneider, G. M. *J. Supercrit. Fluids* **1998**, *13*, 5.
- Villard, P. *Chem. News* **1898**, *78*, 297.
- Kazarian, S. G.; Sakellarios, N.; Gordon, C. M. *Chem. Commun.* **2002**, 1314.
- Hammam, H.; Sivik, B. *J. Supercrit. Fluids* **1993**, *6*, 223.
- Cleve, E.; Bach, E.; Schollmeyer, E. *Angew. Makromol. Chem.* **1998**, *256*, 39.
- Kishimoto, Y.; Ishii, R. *Polymer* **2000**, *41*, 3483.
- Kukova, E.; Petermann, M.; Weidner, E. *Chem.-Ing.-Tech.* **2004**, *76*, 280.
- Liao, X.; Wang, J.; Li, G.; He, J. *J. Polym. Sci., Part B: Polym. Phys.* **2004**, *42*, 280.
- Shenoy, S. L.; Fujiwara, T.; Wynne, K. J. *Macromol. Symp.* **2003**, *201*, 171.
- Shieh, Y.-T.; Liu, K.-H. *J. Polym. Sci., Part B: Polym. Phys.* **2004**, *42*, 2479.
- Shieh, Y.-T.; Yang, H.-S. *J. Supercrit. Fluids* **2005**, *33*, 183.
- McHugh, M. A.; Yogan, T. J. *J. Chem. Eng. Data* **1984**, *29*, 112.
- Diepen, G. A. M.; Scheffer, F. E. C. *J. Am. Chem. Soc.* **1948**, *70*, 4081.
- Paulaitis, M. E.; Kander, R. G.; DiAndreth, J. R. *Ber. Bunsen-Ges.* **1984**, *88*, 869.
- de Loos, T. W. *J. Supercrit. Fluids* **2006**, *39*, 154.
- de Leeuw, V. V.; Poot, W.; de Loos, T. W.; de Swaan Arons, J. *Fluid Phase Equilib.* **1989**, *49*, 75.

- (78) de Swaan Arons, J.; Diepen, G. A. M. *Rec. Trav. Chim. Pays-Bas* **1963**, *82*, 249.
- (79) Niehaus, D. E.; Wightman, R. M. *Anal. Chem.* **1991**, *63*, 1728.
- (80) Leitner, W. Presentation to the 18th Canadian Symposium on Catalysis, Montreal, Canada, May 17, 2004.
- (81) Scurto, A. M.; Leitner, W. *Chem. Commun.* **2006**, 3681.
- (82) Madsen, L. A. *Macromolecules* **2006**, *39*, 1483.
- (83) Varma-Nair, M.; Handa, P. Y.; Mehta, A. K.; Agarwal, P. *Thermo-chim. Acta* **2003**, *396*, 57.
- (84) Takada, M.; Ohshima, M. *Polym. Eng. Sci.* **2003**, *43*, 479.
- (85) Handa, Y. P.; Roovers, J.; Wang, F. *Macromolecules* **1994**, *27*, 5511.
- (86) Sassiati, P. R.; Mourier, P.; Caude, M. H.; Rosset, R. H. *Anal. Chem.* **1987**, *59*, 1164.
- (87) Maxey, N. B. Ph.D. Dissertation, Georgia Institute of Technology, 2006.
- (88) Kho, Y. W.; Conrad, D. C.; Knutson, B. L. *Fluid Phase Equilib.* **2003**, *206*, 179.
- (89) Shiflett, M. B.; Yokozeki, A. *Ind. Eng. Chem. Res.* **2005**, *44*, 4453.
- (90) Shiflett, M. B.; Yokozeki, A. *AIChE J.* **2005**, *52*, 1205.
- (91) Morgan, D.; Ferguson, L.; Scovazzo, P. *Ind. Eng. Chem. Res.* **2005**, *44*, 4815.
- (92) Liu, Z.; Wu, W.; Han, B.; Dong, Z.; Zhao, G.; Jiaqiu Wang; Jiang, T.; Yang, G. *Chem.—Eur. J.* **2003**, *9*, 3897.
- (93) Wissinger, R. G.; Paulaitis, M. E. *J. Polym. Sci. B: Polym. Phys.* **1991**, *29*, 631.
- (94) Condo, P. D.; Sanchez, I. C.; Panayiotou, C. G.; Johnston, K. P. *Macromolecules* **1992**, *25*, 6119.
- (95) Goel, S. K.; Beckman, E. J. *Polymer* **1993**, *34*, 1410.
- (96) Condo, P. D.; Paul, D. R.; Johnston, K. P. *Macromolecules* **1994**, *27*, 365.
- (97) Zhang, Z.; Handa, Y. P. *J. Polym. Sci. B: Polym. Phys.* **1998**, *36*, 977.
- (98) Shenoy, S. L.; Fujiwara, T.; Wynne, K. J. *Polym. Prepr.* **2002**, *43*, 887.
- (99) Gerhardt, L. J.; Manke, C. W.; Gulari, E. *J. Polym. Sci., Part B: Polym. Phys.* **1997**, *35*, 523.
- (100) Tomasko, D. L.; Li, H.; Liu, D.; Han, X.; Wingert, M. J.; Lee, L. J.; Koelling, K. W. *Ind. Eng. Chem. Res.* **2003**, *42*, 6431.
- (101) Nalawade, S. P.; Picchioni, F.; Janssen, L. P. B. M. *Prog. Polym. Sci.* **2006**, *31*, 19.
- (102) Kwag, C.; Manke, C. W.; Gulari, E. *J. Polym. Sci., Part B: Polym. Phys.* **1999**, *37*, 2771.
- (103) Royer, J. R.; Gay, Y. J.; DeSimone, J. M.; Khan, S. A. *J. Polym. Sci., part B: Polym. Phys.* **2000**, *38*, 3168.
- (104) Royer, J. R.; Gay, Y. J.; Adam, M.; DeSimone, J. M.; Khan, S. A. *Polymer* **2002**, *43*, 2375.
- (105) Flichy, N. M. B.; Lawrence, C. J.; Kazarian, S. G. *Ind. Eng. Chem. Res.* **2003**, *42*, 6310.
- (106) Liu, K.; Schuch, F.; Kiran, E. *J. Supercrit. Fluids* **2006**, *39*, 89.
- (107) Lee, M. H.; Tzoganakis, C.; Park, C. B. *Polym. Eng. Sci.* **1998**, *38*, 1112.
- (108) Lee, M.; Tzoganakis, C.; Park, C. B. *Adv. Polym. Technol.* **2000**, *19*, 300.
- (109) Ladin, D.; Park, C. B.; Park, S. S.; Naguib, H. E. *Antek* **2000**, *58*, 1955.
- (110) Royer, J. R.; Gay, Y. J.; DeSimone, J. M.; Khan, S. A. *J. Polym. Sci., B: Polym. Phys.* **2001**, *39*, 3055.
- (111) Lan, H.-Y.; Tseng, H.-C. *J. Polym. Res.* **2002**, *9*, 157.
- (112) Xue, A.; Tzoganakis, C. *J. Polym. Eng.* **2003**, *23*, 1.
- (113) Whittier, R. E.; Xu, D.; van Zanten, J. H.; Kiserow, D. J.; Roberts, G. W. *J. Appl. Polym. Sci.* **2005**, *99*, 540.
- (114) Sarrade, S.; Schrive, L.; Gourguillon, D.; Rios, G. M. *Sep. Purif. Technol.* **2001**, *25*, 315.
- (115) Hsu, J. J. C.; Nagarajan, N.; Robinson, Jr., R. L. *J. Chem. Eng. Data* **1985**, *30*, 485.
- (116) Kanakubo, M.; Umecky, T.; Aizawa, T.; Ikushima, Y. *Electrochemistry (Tokyo)* **2004**, *72*, 703.
- (117) Tominaga, Y.; Hirahara, S.; Asai, S.; Sumita, M. *Polymer* **2005**, *46*, 8113.
- (118) Toews, K. L.; Shroll, R. M.; Wai, C. M.; Smart, N. G. *Anal. Chem.* **1995**, *67*, 4040.
- (119) Bonilla, R. J.; James, B. R.; Jessop, P. G. *Chem. Commun.* **2000**, 941.
- (120) Roosen, C.; Ansoorge-Schumacher, M.; Mang, T.; Leitner, W.; Greiner, L. *Green Chem.* **2007**, 455.
- (121) Hunter, S. E.; Savage, P. E. *Ind. Eng. Chem. Res.* **2003**, *42*, 290.
- (122) West, K. N.; Wheeler, C.; McCarney, J. P.; Griffith, K. N.; Bush, D.; Liotta, C. L.; Eckert, C. A. *J. Phys. Chem. A* **2001**, *105*, 3947.
- (123) Ganchevui, B.; Leitner, W. *Green Chem.* **2007**, *9*, 26.
- (124) Liu, D. X.; Zhang, J. L.; Han, B. X.; Fan, J. F.; Mu, T. C.; Liu, Z. M.; Wu, W. Z.; Chen, J. *J. Chem. Phys.* **2003**, *119*, 4873.
- (125) Mendez-Santiago, J.; Teja, A. S. *Ind. Eng. Chem. Res.* **2000**, *39*, 4767.
- (126) Dobbs, J. M.; Johnston, K. P. *Ind. Eng. Chem. Res.* **1987**, *26*, 1476.
- (127) Harvey, A. H. *J. Phys. Chem.* **1990**, *94*, 8403.
- (128) Jin, H.; Subramaniam, B.; Ghosh, A.; Tunge, J. *AIChE J.* **2006**, *52*, 2575.
- (129) Kaminishi, G.; Arai, Y.; Saito, S.; Maeda, S. *J. Chem. Eng. Jpn.* **1968**, *1*, 109.
- (130) Christiansen, L. J.; Fredenslund, A.; Gardner, N. *Adv. Cryog. Eng.* **1974**, *19*, 309.
- (131) Dyson, P. J.; Laurencyzy, G.; Ohlin, C. A.; Vallance, J.; Welton, T. *Chem. Commun.* **2003**, 2418.
- (132) Hert, D. G.; Anderson, J. L.; Aki, S. N. V. K.; Brennecke, J. F. *Chem. Commun.* **2005**, 2603.
- (133) Solinas, M.; Pfaltz, A.; Cozzi, P. G.; Leitner, W. *J. Am. Chem. Soc.* **2004**, *126*, 16142.
- (134) Bezanehtak, K.; Dehghani, F.; Foster, N. R. *J. Chem. Eng. Data* **2004**, *49*, 430.
- (135) Xie, X. F.; Brown, J. S.; Bush, D.; Eckert, C. A. *J. Chem. Eng. Data* **2005**, *50*, 780.
- (136) Lopez-Castillo, Z. K.; Aki, S. N. V. K.; Stadtherr, M. A.; Brennecke, J. F. *Ind. Eng. Chem. Res.* **2006**, *45*, 5351.
- (137) Musie, G.; Wei, M.; Subramaniam, B.; Busch, D. H. *Coord. Chem. Rev.* **2001**, *219*, 789.
- (138) Adrian, T.; Maurer, G. In *High Pressure Chemical Engineering: Proceedings of the 3rd International Symposium on High Pressure Chemical Engineering, Zurich, Switzerland, 7–9 October, 1996*; von Rohr, P. R.; Trepp, C., Eds.; Elsevier: Amsterdam, 1996.
- (139) Efremova, G. D.; Shvarts, A. V. *Russ. J. Phys. Chem.* **1966**, *40*, 486.
- (140) Wendland, M.; Hasse, H.; Maurer, G. *J. Supercrit. Fluids* **1993**, *6*, 211.
- (141) Adrian, T.; Freitag, J.; Maurer, G. *Fluid Phase Equilib.* **1999**, *158–160*, 685.
- (142) Scurto, A. M.; Aki, S.; Brennecke, J. F. *J. Am. Chem. Soc.* **2002**, *124*, 10276.
- (143) Aki, S. N. V. K.; Scurto, A. M.; Brennecke, J. F. *Ind. Eng. Chem. Res.* **2006**, *45*, 5574.
- (144) Zhang, Z.; Wu, W.; Gao, H.; Han, B.; Wang, B.; Huang, Y. *Phys. Chem. Chem. Phys.* **2004**, *6*, 5051.
- (145) Wendland, M.; Hasse, H.; Maurer, G. *J. Supercrit. Fluids* **1994**, *7*, 245.
- (146) Laugier, S.; Richon, D.; Renon, H. *Fluid Phase Equilib.* **1990**, *54*, 19.
- (147) Panagiotopoulos, A. Z.; Willson, R. C.; Reid, R. C. *J. Chem. Eng. Data* **1988**, *33*, 321.
- (148) Adrian, T.; Hasse, H.; Maurer, G. *J. Supercrit. Fluids* **1996**, *9*, 19.
- (149) Lu, J.; Lazzaroni, M. J.; Hallett, J. P.; Bommarius, A. S.; Liotta, C. L.; Eckert, C. A. *Ind. Eng. Chem. Res.* **2004**, *43*, 1586.
- (150) Lazzaroni, M. J.; Bush, D.; Jones, R.; Hallett, J. P.; Liotta, C. L.; Eckert, C. A. *Fluid Phase Equilib.* **2004**, *224*, 143.
- (151) Gerritsen, H.-G.; Hartmann, H. *Chem.-Ing.-Tech.* **1979**, *51*, 303.
- (152) Zhang, Z.; Wu, W.; Liu, Z.; Han, B.; Gao, H.; Jiang, T. *Phys. Chem. Chem. Phys.* **2004**, *6*, 2352.
- (153) Adrian, T.; Wendland, M.; Hasse, H.; Maurer, G. *J. Supercrit. Fluids* **1998**, *12*, 185.
- (154) Elgin, J. C.; Weinstock, J. J. *J. Chem. Eng. Data* **1959**, *4*, 3.
- (155) Catchpole, O. J.; Hochmann, S.; Anderson, S. R. J. In *High Pressure Chemical Engineering: Proceedings of the 3rd International Symposium on High Pressure Chemical Engineering, Zurich, Switzerland, 7–9 October, 1996*; von Rohr, P. R.; Trepp, C., Eds.; Elsevier: Amsterdam, 1996.
- (156) Pfohl, O.; Dohrn, R.; Brunner, G. In *High Pressure Chemical Engineering: Proceedings of the 3rd International Symposium on High Pressure Chemical Engineering, Zurich, Switzerland, 7–9 October, 1996*; von Rohr, P. R.; Trepp, C., Eds.; Elsevier: Amsterdam, 1996.
- (157) Pfohl, O.; Petersen, J.; Dohrn, R.; Brunner, G. *J. Supercrit. Fluids* **1997**, *10*, 95.
- (158) Pfohl, O.; Timm, J.; Dohrn, R.; Brunner, G. *Fluid Phase Equilib.* **1996**, *124*, 221.
- (159) Adrian, T.; Freitag, J.; Maurer, G. *J. Supercrit. Fluids* **2000**, *17*, 197.
- (160) West, K. N.; Hallett, J. P.; Jones, R. S.; Bush, D.; Liotta, C. L.; Eckert, C. A. *Ind. Eng. Chem. Res.* **2004**, *43*, 4827.
- (161) Draucker, L. C.; Hallett, J. P.; Bush, D.; Eckert, C. A. *Fluid Phase Equilib.* **2006**, *241*, 20.
- (162) Kho, Y. W.; Conrad, D. C.; Knutson, B. L. *Langmuir* **2004**, *20*, 2590.
- (163) *Modeling Vapor-Liquid Equilibria: Cubic Equations of State and Their Mixing Rules*; Orbey, H.; Sandler, S., Eds.; Cambridge University Press: Cambridge, U.K., 1998.
- (164) *Equations of State for Fluids and Fluid Mixtures*; Sengers, J. V.; Kayser, R. F.; Peters, C. J.; White, J., H. J., Eds.; Elsevier: Amsterdam, 2000.
- (165) Peng, D.; Robinson, D. *Ind. Eng. Chem. Fund.* **1976**, *15*, 59.
- (166) Cassel, E.; Matt, M.; Rogalski, M.; Solimando, R. *Fluid Phase Equilib.* **1997**, *134*, 63.

- (167) Frink, L. J. D.; Martin, M. *Condens. Matter Phys.* **2005**, *8*, 271.
- (168) Panagiotopoulos, A. Z. *Fluid Phase Equilib.* **1992**, *76*, 97.
- (169) Ferrenberg, A.; Swendsen, R. *Phys. Rev. Lett.* **1988**, *61*, 2635.
- (170) Ferrenberg, A.; Swendsen, R. *Phys. Rev. Lett.* **1989**, *63*, 1195.
- (171) Potoff, J. J.; Errington, J. R.; Panagiotopoulos, A. Z. *Mol. Phys.* **1999**, *97*, 1073.
- (172) Kofke, D. A. *J. Chem. Phys.* **1993**, *98*, 4149.
- (173) Shah, J. K.; Maginn, E. J. *J. Phys. Chem. B* **2005**, *109*, 10395.
- (174) Adrian, T.; Maurer, G. *J. Chem. Eng. Data* **1997**, *42*, 668.
- (175) Woerlee, G. F. *Ind. Eng. Chem. Res.* **2001**, *40*, 465.
- (176) Gerhardt, L. J.; Garg, A.; Manke, C. W.; Gulari, E. J. *Polym. Sci., Part B: Polym. Phys.* **1998**, *36*, 1911.
- (177) Doolittle, A. K. *J. Appl. Phys.* **1951**, *22*, 1471.
- (178) Kwag, C.; Manke, C. W.; Gulari, E. *Ind. Eng. Chem. Res.* **2001**, *40*, 3048.
- (179) Lin, C.; Muhrer, G.; Mazzotti, M.; Subramaniam, B. *Ind. Eng. Chem. Res.* **2003**, *42*, 2171.
- (180) Fusaro, F.; Hänchen, M.; Mazzotti, M.; Muhrer, G.; Subramaniam, B. *Ind. Eng. Chem. Res.* **2005**, *44*, 1502.
- (181) Guha, D.; Jin, H.; Dudukovic, M. P.; Ramachandran, P. A.; Subramaniam, B. *Chem. Eng. Sci.* **2007**, in press.
- (182) Jin, H.; Subramaniam, B. *Chem. Eng. Sci.* **2004**, *59*, 4887.
- (183) Jung, J.; Perrut, M. *J. Supercrit. Fluids* **2001**, *20*, 179.
- (184) Fages, J.; Lochar, H.; Letourneau, J.-J.; Sauceau, M.; Rodier, E. *Powder Technol.* **2004**, *141*, 219.
- (185) Yeo, S.-D.; Kiran, E. *J. Supercrit. Fluids* **2005**, *34*, 287.
- (186) Graser, F.; Wickenhaeuser, G.; BASF: U.S. 4,451,654, 1982 (CAN 101:92903).
- (187) Kokot, K.; Knez, Z.; Bauman, D. *Acta Aliment.* **1999**, *28*, 197.
- (188) Pourmortazavi, S. M.; Hajimirsadeghi, S. S. *Ind. Eng. Chem. Res.* **2005**, *44*, 6523.
- (189) Bertucco, A. In *Chemical Synthesis Using Supercritical Fluids*; Jessop, P. G.; Leitner, W., Eds.; Wiley-VCH: Weinheim, Germany, 1999.
- (190) Palakodaty, S.; York, P. *Pharm. Res.* **1999**, *16*, 976.
- (191) *Merck Index*, 12th ed.; Budavari, S.; O'Neil, M. J.; Smith, A.; Heckelman, P. E.; Kinneary, J. F., Eds.; Merck & Co., Inc.: Whitehouse Station, NJ, 1996.
- (192) Sencar-Bozic, P.; Srcic, S.; Knez, Z.; Kerc, J. *Int. J. Pharm.* **1997**, *148*, 123.
- (193) Shine, A.; Gelb, J. WO Patent 98/15348, 1998.
- (194) Krukoni, V. J.; Gallagher, P. M.; Coffey, M. P. U.S. Patent 5,360,478, 1994 (application 1991, CAN 122:34594).
- (195) Field, C. N.; Hamley, P. A.; Webster, J. M.; Gregory, D. H.; Titman, J. J.; Poliakoff, M. *J. Am. Chem. Soc.* **2000**, *122*, 2480.
- (196) O'Neil, A.; Wilson, C.; Webster, J. M.; Allison, F. J.; Howard, J. A. K.; Poliakoff, M. *Angew. Chem., Int. Ed.* **2002**, *41*, 3796.
- (197) Bleich, J.; Müller, B. W.; Wassmus, W. *Int. J. Pharm.* **1993**, *97*, 111.
- (198) Hutchings, G. J.; Bartley, J. K.; Webster, J. M.; Lopez-Sanchez, J. A.; Gilbert, D. J.; Kiely, C. J.; Carley, A. F.; Howdle, S. M.; Sajip, S.; Caldarelli, S.; Rhodes, C.; Volta, J. C.; Poliakoff, M. *J. Catal.* **2001**, *197*, 232.
- (199) Johnson, C. A.; Sharma, S.; Subramaniam, B.; Borovik, A. S. *J. Am. Chem. Soc.* **2005**, *127*, 9698.
- (200) Hanna, M.; York, P. WO Patent 95/01221 A1, 1994 (AN 2005:769844).
- (201) Subramaniam, B.; Saim, S.; Rajewski, R. A.; Stella, V. J. In *Green Engineering*; Anastas, P. T., Heine, L. G., Williamson, T. C., Eds.; Oxford University Press: Washington, D.C., 2000.
- (202) Snavelly, W. K.; Subramaniam, B.; Rajewski, R. A.; DeFelippis, M. R. *J. Pharm. Sci.* **2002**, *91*, 2026.
- (203) Niu, F.; Roby, K. F.; Rajewski, R. A.; Decedue, C.; Subramaniam, B. In *Polymeric Drug Delivery Volume II—Polymeric Matrices and Drug Particle Engineering*; Svenson, S., Ed.; Oxford University Press: Washington, DC, 2006.
- (204) Ventosa, N.; Sala, S.; Veciana, J.; Torres, J.; Llibre, J. *Cryst. Growth Des.* **2001**, *1*, 299.
- (205) Ventosa, N.; Sala, S.; Veciana, J. *J. Supercrit. Fluids* **2003**, *26*, 33.
- (206) Gimeno, M.; Ventosa, N.; Sala, S.; Veciana, J. *Cryst. Growth Des.* **2006**, *6*, 23.
- (207) Chen, J.; Zhang, J. L.; Liu, D. X.; Liu, Z. M.; Han, B. X.; Yang, G. Y. *Colloids Surf., B* **2004**, *33*, 33.
- (208) Zhang, H. F.; Lu, J.; Han, B. X. *J. Supercrit. Fluids* **2001**, *20*, 65.
- (209) Zhang, J. L.; Han, B. X.; Liu, J. C.; Zhang, X. G.; He, J.; Liu, Z. M. *Chem. Commun.* **2001**, 2724.
- (210) Zhang, J. L.; Han, B. X.; Liu, J. C. *Chem.—Eur. J.* **2002**, *8*, 3879.
- (211) Anand, M.; McLeod, M. C.; Bell, P. W.; Roberts, C. B. *J. Phys. Chem. B* **2005**, *109*, 22852.
- (212) McLeod, M. C.; Anand, M.; Kitchens, C. L.; Roberts, C. B. *Nano Lett.* **2005**, *5*, 461.
- (213) McLeod, M. C.; Kitchens, C. L.; Roberts, C. B. *Langmuir* **2005**, *21*, 2414.
- (214) Liu, J.; Anand, M.; Roberts, C. B. *Langmuir* **2006**, *22*, 3964.
- (215) Subramaniam, B.; Saim, S.; Rajewski, R.; Stella, V. J. U.S. Patent 5,833,891; 1998 (CAN 129:347344).
- (216) Borchardt, J. K. In *Kirk-Othmer Encyclopedia of Chemical Technology*, 4th ed.; Kroschwitz, J. I.; Howe-Grant, M., Eds.; Wiley: New York, 1996; Vol. 18.
- (217) Hwang, R. J.; Ortiz, J. *Org. Geochem.* **2000**, *31*, 1451.
- (218) Kovscek, A. R.; Cakici, M. D. *Energy Convers., Manage.* **2005**, *46*, 1941.
- (219) Beeson, D. M.; Orloff, G. D. *J. Petrol. Technol.* **1959**, *11*, 63.
- (220) Welker, J. R.; Dunlop, D. D. *J. Petrol. Technol.* **1963**, *15*, 873.
- (221) Killesreiter, H. *Ber. Bunsen-Ges.* **1984**, *88*, 838.
- (222) Simon, R.; Graue, D. J. *J. Petrol. Technol.* **1965**, *17*, 102.
- (223) Shelton, J. L.; Yarborough, L. J. *J. Petrol. Technol.* **1977**, 1171.
- (224) Worden, R. H.; Smith, L. K. In *Geological Storage of Carbon Dioxide*; Baines, S. J.; Worden, R. H., Eds.; Geological Society Special Publication 233, Geological Society Publishing House: London, 2004.
- (225) Handa, Y. P.; Zhang, Z.; Roovers, J. *J. Polym. Sci., Part B: Polym. Phys.* **2001**, *39*, 1505.
- (226) Verreck, G.; Decorte, A.; Li, H.; Tomasko, D.; Arien, A.; Peeters, J.; Rombaut, P.; Van den Mooter, G.; Brewster, M. E. *J. Supercrit. Fluids* **2006**, *38*, 383.
- (227) Beckman, E.; Porter, R. S. *J. Polym. Sci., Part B: Polym. Phys.* **1987**, *25*, 1511.
- (228) Gross, S. M.; Roberts, G. W.; Kiserow, D. J.; DeSimone, J. M. *Macromolecules* **2000**, *33*, 40.
- (229) Handa, Y. P.; Capowski, S.; O'Neill, M. *Thermochim. Acta* **1993**, *226*, 177.
- (230) Lambert, S. M.; Paulaitis, M. E. *J. Supercrit. Fluids* **1991**, *4*, 15.
- (231) Schultze, J. D.; Engelman, I. A. D.; Boehning, M.; Springer, J. *Polym. Adv. Technol.* **1991**, *2*, 123.
- (232) Handa, Y. P.; Zhang, Z.; Wong, B. *Macromolecules* **1997**, *30*, 8499.
- (233) Zhang, Z.; Handa, Y. P. *Macromolecules* **1997**, *30*, 8505.
- (234) Shenoy, S. L.; Fujiwara, T.; Wynne, K. *PMSE [Prepr.]* **2003**, *89*, 763.
- (235) Shieh, Y.-T.; Lin, Y.-G.; Chen, H.-L. *Polymer* **2002**, *43*, 3691.
- (236) Teramoto, G.; Oda, T.; Saito, H.; Sano, H.; Fujita, Y. *J. Polym. Sci., Part B: Polym. Phys.* **2004**, *42*, 2738.
- (237) Kropp, D. Hermann Berstorff Maschinenbau GmbH, Germany: Eur. Pat. Appl., 1997.
- (238) Nagata, T.; Areerat, S.; Ohshima, M.; Tanigaki, M. *Kagaku Kagaku Ronbunshu* **2002**, *28*, 739.
- (239) Maeda, T.; Otake, K.; Nakayama, K.; Horiuchi, S.; Sanyo Electric Co., Ltd., Japan; National Institute of Advanced Industrial Science and Technology: Jpn. Kokai Tokkyo Koho, Japan, 2003.
- (240) Bortner, M. J.; Baird, D. G. *Polymer* **2004**, *45*, 3399.
- (241) Howdle, S. M.; Watson, M. S.; Whitaker, M. J.; Popov, V. K.; Davies, M. C.; Mandel, F. S.; Wang, J. D.; Shakesheff, K. M. *Chem. Commun.* **2001**, 109.
- (242) McHugh, M. A.; Wang, J. D.; Mandel, F. S. In *Supercritical Fluid Technology in Materials Science: Synthesis, Properties, and Applications*; Sun, Y. P., Ed.; Marcel Dekker: New York, 2002.
- (243) Cooper, A. I. *J. Mater. Chem.* **2000**, *10*, 207.
- (244) Jessop, P. G.; Olmstead, M. M.; Ablan, C. D.; Grabenauer, M.; Sheppard, D.; Eckert, C. A.; Liotta, C. L. *Inorg. Chem.* **2002**, *41*, 3463.
- (245) Jessop, P. G.; Ablan, C. D.; Eckert, C. A.; Liotta, C. L. In *Handbook of Fluorous Chemistry*; Gladysz, J. A., Curran, D. P., Horváth, I. T., Eds.; Wiley-VCH: Weinheim, Germany, 2004.
- (246) Shshikura, A.; Kanamori, K.; Takahashi, H.; Kinbara, H. *J. Agric. Food Chem.* **1994**, *42*, 1993.
- (247) Chang, C. J.; Randolph, A. D. *Biotechnol. Progr.* **1991**, *7*, 275.
- (248) Wen, D.; Olesik, S. V. *Anal. Chim. Acta* **2001**, *449*, 211.
- (249) Wen, D.; Olesik, S. V. *J. Chromatogr., A* **2001**, *931*, 41.
- (250) Lee, S. T.; Olesik, S. V.; Fields, S. M. *J. Microcolumn Sep.* **1995**, *7*, 477.
- (251) Yuan, H. M.; Olesik, S. V. *Anal. Chem.* **1998**, *70*, 1595.
- (252) Zhao, J.; Olesik, S. V. *J. Chromatogr., A* **2001**, *923*, 107.
- (253) Yuan, H. M.; Olesik, S. V. *J. Chromatogr., A* **1997**, *785*, 35.
- (254) Yuan, H. M.; Souvignat, I.; Olesik, S. V. *J. Chromatogr. Sci.* **1997**, *35*, 409.
- (255) Yun, H.; Olesik, S. V.; Marti, E. H. *Anal. Chem.* **1998**, *70*, 3298.
- (256) Zhao, J.; Olesik, S. V. *Anal. Chim. Acta* **2001**, *449*, 221.
- (257) Sun, Q.; Olesik, S. V. *Anal. Chem.* **1999**, *71*, 2139.
- (258) Sun, Q.; Olesik, S. V. *J. Chromatogr., B* **2000**, *745*, 159.
- (259) Musie, G. T.; Wei, M.; Subramaniam, B.; Busch, D. H. *Inorg. Chem.* **2001**, *40*, 3336.
- (260) The TOF values in Table 3 of that reference are reversed. The text is correct.
- (261) Ablan, C. D.; Hallett, J. P.; West, K. N.; Jones, R. S.; Eckert, C. A.; Liotta, C. L.; Jessop, P. G. *Chem. Commun.* **2003**, 2972.
- (262) Downing, R. C. *Fluorocarbon Refrigerants Handbook*; Prentice Hall: Englewood Cliffs, NJ, 1988.

- (263) Sutter, H.; Cole, R. H. *J. Chem. Phys.* **1970**, *52*, 132.
- (264) Fernández, D. P.; Mulev, Y.; Goodwin, A. R. H.; Levelt Sengers, J. M. H. *J. Phys. Chem. Ref. Data* **1995**, *24*, 33.
- (265) Franck, E. U.; Deul, R. *Faraday Discuss. Chem. Soc.* **1978**, *66*, 191.
- (266) Wynne, D.; Jessop, P. G. *Angew. Chem., Int. Ed.* **1999**, *38*, 1143.
- (267) Wynne, D.; Olmstead, M. M.; Jessop, P. G. *J. Am. Chem. Soc.* **2000**, *122*, 7638.
- (268) Phan, L.; Li, X.; Heldebrant, D. J.; Wang, R.; Chiu, D.; John, E.; Huttenhower, H.; Pollet, P.; Eckert, C. A.; Liotta, C. L.; Jessop, P. G., submitted for publication, 2007.
- (269) Yamada, T.; Lukac, P. J.; George, M.; Weiss, R. G. *Chem. Mater.* **2007**, *19*, 967.
- (270) Phan, L.; Horvey, L. K.; Edie, C. F.; Jessop, P. G.; Darensbourg, D. J., manuscript in preparation, 2007.
- (271) Eckert, C.; Jessop, P. G.; Liotta, C. U.S. Provisional Application, 2001.
- (272) Warwick, B.; Dehghani, F.; Foster, N. R.; Biffin, J. R.; Regtop, H. L. *Ind. Eng. Chem. Res.* **2000**, *39*, 4571.
- (273) Blanchard, L. A.; Brennecke, J. F. *Green Chem.* **2001**, *3*, 17.
- (274) Dunetz, J. R.; Ciccolini, R. P.; Fröling, M.; Paap, S. M.; Allen, A. J.; Holmes, A. B.; Tester, J. W.; Danheiser, R. L. *Chem. Commun.* **2005**, 4465.
- (275) Liu, J.; Han, B.; Liu, Z.; Wang, J.; Huo, Q. *J. Supercrit. Fluids* **2001**, *20*, 171.
- (276) Liu, J.; Han, B.; Zhang, R.; Liu, Z.; Jiang, T.; Yang, G. *J. Supercrit. Fluids* **2003**, *25*, 91.
- (277) Xu, Q.; Han, B.; Yan, H. *J. Appl. Polym. Sci.* **2003**, *88*, 2427.
- (278) Price, G. J. *Ultrason. Sonochem.* **1996**, *3*, S229.
- (279) Kemmere, M. F.; Kuijpers, M. W. A.; Prickaerts, R. M. H.; Keurentjes, J. T. F. *Macromol. Mater. Eng.* **2005**, *290*, 302.
- (280) Kuijpers, M. W. A.; Jacobs, L. J. M.; Kemmere, M. F.; Keurentjes, J. T. F. *AIChE J.* **2005**, *51*, 1726.
- (281) Noyori, R. *Asymmetric Catalysis in Organic Synthesis*; John Wiley and Sons: New York, 1994.
- (282) Sun, Y.; Landau, R. N.; Wang, J.; LeBlond, C.; Blackmond, D. G. *J. Am. Chem. Soc.* **1996**, *118*, 1348.
- (283) Combes, G. B.; Dehghani, F.; Lucien, F. P.; Dillow, A. K.; Foster, N. R. In *Reaction Engineering for Pollution Prevention*; Abraham, M. A.; Hesketh, R. P., Eds.; Elsevier: Amsterdam, 2000.
- (284) Significant problems were experienced with catalyst deactivation in this study; it is uncertain to what extent this may have affected the results.
- (285) Combes, G.; Coen, E.; Dehghani, F.; Foster, N. *J. Supercrit. Fluids* **2005**, *36*, 127.
- (286) Anthony, J. L.; Maginn, E. J.; Brennecke, J. F. *J. Phys. Chem. B* **2002**, *106*, 7315.
- (287) Jessop, P. G.; Stanley, R.; Brown, R. A.; Eckert, C. A.; Liotta, C. L.; Ngo, T. T.; Pollet, P. *Green Chem.* **2003**, *5*, 123.
- (288) Monteiro, A. L.; Zinn, F. K.; DeSouza, R. F.; Dupont, J. *Tetrahedron: Asymmetry* **1997**, *8*, 177.
- (289) Xie, X.; Liotta, C. L.; Eckert, C. A. *Ind. Eng. Chem. Res.* **2004**, *43*, 7907.
- (290) Jessop, P. G.; DeHaai, S.; Wynne, D. C.; Nakawatase, D. *Chem. Commun.* **2000**, 693.
- (291) Hemminger, O.; Marteel, A.; Mason, M. R.; Davies, J. A.; Tadd, A. R.; Abraham, M. A. *Green Chem.* **2002**, *V4*, 507.
- (292) Francio, G.; Wittmann, K.; Leitner, W. *J. Organomet. Chem.* **2001**, *621*, 130.
- (293) Sellin, M. F.; Webb, P. B.; Cole-Hamilton, D. J. *Chem. Commun.* **2001**, 781.
- (294) Webb, P. B.; Kunene, T. E.; Cole-Hamilton, D. J. *Green Chem.* **2005**, *7*, 373.
- (295) Webb, P. B.; Sellin, M. F.; Kunene, T. E.; Williamson, S.; Slawin, A. M. Z.; Cole-Hamilton, D. J. *J. Am. Chem. Soc.* **2003**, *125*, 15577.
- (296) Wei, M.; Musie, G. T.; Busch, D. H.; Subramaniam, B. *Green Chem.* **2004**, *6*, 387.
- (297) Yao, H.; Richardson, D. E. *J. Am. Chem. Soc.* **2000**, *122*, 3220.
- (298) Thiele, G.; Nolan, S. A.; Brown, J. S.; Lu, J.; Eason, B. C.; Eckert, C. A.; Liotta, C. L. U.S. Patent 6,100,412; 2000 (CAN 133:120228).
- (299) Nolen, S. A.; Lu, J.; Brown, J. S.; Pollet, P.; Eason, B. C.; Griffith, K. N.; Glaser, R.; Bush, D.; Lamb, D. R.; Liotta, C. L.; Eckert, C. A.; Thiele, G. F.; Bartels, K. A. *Ind. Eng. Chem. Res.* **2002**, *41*, 316.
- (300) Hancu, D.; Green, J.; Beckman, E. J. *Acc. Chem. Res.* **2002**, *35*, 757.
- (301) Beckman, E. J. *Green Chem.* **2003**, *5*, 332.
- (302) Lee, H.-J.; Shi, T.-P.; Subramaniam, B.; Busch, D. H. In *Catalysis of Organic Reactions*; Schmidt, S. R., Ed.; CRC Press: Boca Raton, FL, 2006.
- (303) Zwolak, G.; Jayasinghe, N. S.; Lucien, F. P. *J. Supercrit. Fluids* **2006**, *38*, 420.
- (304) Baiker, A. *Chem. Rev.* **1999**, *99*, 453.
- (305) Subramaniam, B.; Busch, D. H. In *Carbon Dioxide Conversion and Utilization*; Song, C.; Gaffney, A. F.; Fujimoto, K., Eds.; American Chemical Society: Washington, DC, 2002.
- (306) Grunwaldt, J. D.; Wandeler, R.; Baiker, A. *Catal. Rev.-Sci. Eng.* **2003**, *45*, 1.
- (307) Beckman, E. J. *J. Supercrit. Fluids* **2004**, *28*, 121.
- (308) Xu, D.; Carbonell, R. G.; Kiserow, D. J.; Roberts, G. W. *Ind. Eng. Chem. Res.* **2005**, *44*, 6164.
- (309) Devetta, L.; Giovanzana, A.; Canu, P.; Bertucco, A.; Minder, B. *J. Catal. Today* **1999**, *48*, 337.
- (310) Chouchi, D.; Gourguillon, D.; Courel, M.; Vital, J.; da Ponte, M. N. *Ind. Eng. Chem. Res.* **2001**, *40*, 2551.
- (311) Jenzer, G.; Schneider, M. S.; Wandeler, R.; Mallat, T.; Baiker, A. *J. Catal.* **2001**, *199*, 141.
- (312) Chan, J. C.; Tan, C. S. *Energy Fuels* **2006**, *20*, 771.
- (313) Fürstner, A.; Koch, D.; Langemann, K.; Leitner, W.; Six, C. *Angew. Chem., Int. Ed. Engl.* **1997**, *36*, 2466.
- (314) Wittmann, K.; Wisniewski, W.; Mynott, R.; Leitner, W.; Kranemann, C. L.; Rische, T.; Eilbracht, P.; Kluwer, S.; Ernsting, J. M.; Elsevier, C. L. *Chem.-Eur. J.* **2001**, *7*, 4584.
- (315) Kerler, B.; Robinson, R. E.; Borovik, A. S.; Subramaniam, B. *Appl. Catal., B* **2004**, *49*, 91.
- (316) Sharma, S.; Kerler, B.; Subramaniam, B.; Borovik, A. S. *Green Chem.* **2006**, *8*, 972.
- (317) Sarsani, V. S. R.; Lyon, C. J.; Hutchenson, K. W.; Harmer, M. A.; Subramaniam, B. *J. Catal.* **2007**, *245*, 184.
- (318) Chateaufneuf, J. E.; Nie, K. *Adv. Environ. Res.* **2000**, *4*, 307.
- (319) Xie, X.; Liotta, C. L.; Eckert, C. A. *Ind. Eng. Chem. Res.* **2004**, *43*, 2605.
- (320) Chumblee, T. S.; Weikel, R. R.; Nolen, S. A.; Liotta, C. L.; Eckert, C. A. *Green Chem.* **2004**, *6*, 382.
- (321) Alemán, P. A.; Boix, C.; Poliakkoff, M. *Green Chem.* **1999**, *1*, 65.
- (322) Hunter, S. E.; Savage, P. E. *Chem. Eng. Sci.* **2004**, *59*, 4903.
- (323) Shell Internationale Research Maatschappij N. V.: Patent Application NL 6,906,111; 1969 (CAN 72:45806).
- (324) Little, J. L. *Refriger. Eng.* **1952**, *60*, 1191.
- (325) Spuller, M. T.; Hess, D. W.; Georgia Tech Research Corp.: U.S. Patent 6,786,977 B2, 2004 (CAN 141:32265).
- (326) Perrut, M. *Ind. Eng. Chem. Res.* **2000**, *39*, 4531.
- (327) McHardy, J.; Sawan, S. P. *Supercritical Fluid Cleaning*; William Andrew Publishing: Norwich, 1998.
- (328) O'Neil, A.; Watkins, J. J. *MRS Bull.* **2005**, *30*, 967.
- (329) Mount, D. J.; Rothman, L. B.; Robey, R. J. *Solid State Technol.* **2002**, *45*, 103.
- (330) McCoy, M. *Chem. Eng. News* **1999**, *77* (23), 11.
- (331) Fang, J.; Jin, H.; Ruddy, T.; Pennybaker, K.; Fahey, D.; Subramaniam, B. *Ind. Eng. Chem. Res.* **2007**, submitted for publication.
- (332) *Rhodium Catalyzed Hydroformylation*; Leeuwen, P. W. N. M. v., Claver, C., Eds.; Kluwer Academic Publishers: Boston, MA, 2000.
- (333) Hanin, J. A. A.; Exxon: U.S. Patent 4,658,068, 1987.
- (334) Beckers, H. J.; Rijke, J. M. D.; Garton, R. D. U.S. Patent 5,763,678, 1998.
- (335) Leeuwen, P. W. N. M. v.; Challa, T. J. G. *Macromol. Symp.* **1994**, *80*, 241.
- (336) Shonnard, D. R. In *Green Engineering: Environmentally Conscious Design of Chemical Processes*; Allen, D. T.; Shonnard, D. R., Eds.; Prentice Hall: Upper Saddle River, NJ, 2002.
- (337) Sander, W. Z. *Phys. Chem., Stoichiomet. Verwandtschaftsfl.* **1911–1912**, *78*, 513.
- (338) Wyatt, V. T.; Bush, D.; Lu, J.; Hallett, J. P.; Liotta, C. L.; Eckert, C. A. *J. Supercrit. Fluids* **2005**, *36*, 16.
- (339) Lamb, D. M.; Barbara, T. M.; Jonas, J. J. *Phys. Chem.* **1986**, *90*, 4210.
- (340) van Welie, G. S. A.; Diepen, G. A. M. *J. Phys. Chem.* **1963**, *67*, 755.
- (341) van Gunst, C. A.; Scheffer, F. E. C.; Diepen, G. A. M. *J. Phys. Chem.* **1953**, *57*, 578.
- (342) Hest, J. A. M. V.; Diepen, G. A. M. *Symp. Soc. Chem. Ind. London* **1963**, 10.
- (343) Krukonis, V. J.; McHugh, M. A.; Seckner, A. J. *J. Phys. Chem.* **1984**, *88*, 2687.